EVALUATION OF ABSORPTION
CYCLE FOR SPACE STATION
ENVIRONMENTAL CONTROL
SYSTEM APPLICATION

INTERIM REPORT

March 1971

CASE FILE
COPY

Lockheed

HUNTSVILLE RESEARCH & ENGINEERING CENTER

LOCKHEED MISSILES & SPACE COMPANY
A GROUP DIVISION OF LOCKHEED AIRCRAFT CORPORATION
HUNTSVILLE, ALABAMA

LOCKHEED MISSILES & SPACE COMPANY

HUNTSVILLE RESEARCH & ENGINEERING CENTER

HUNTSVILLE RESEARCH PARK

4800 BRADFORD DRIVE, HUNTSVILLE, ALABAMA

EVALUATION OF ABSORPTION CYCLE FOR SPACE STATION ENVIRONMENTAL CONTROL SYSTEM APPLICATION

INTERIM REPORT

March 1971

Contract NAS8-25986

by

D.V. Hale

J. Thoenes

C.K. Liu

APPROVED: _____

Juan K. Lovin, Supervisor
Thermal Environment Section

_____

George D. Reny, Manager
Aeromechanics Dept.

_____

J.S. Farrior
Resident Director

FOREWORD

This report represents the results of work performed jointly by Lockheed's Huntsville Research & Engineering Center, and Engineering Sciences Laboratory, Palo Alto, California, for the NASA-Marshall Space Flight Center, Alabama, under Exhibit A of Contract NAS8-25986.

Dr. Lynn D. Russell, Director of Engineering, University of Tennessee in Chattanooga, served as a consultant on the study.

The NASA contract monitor for the study was Mr. R.L. Middleton of the MSFC Astronautics Laboratory.

SUMMARY

Studies have shown the need for refrigeration systems to provide low temperatures in manned spacecraft. This is particularly true for adverse orientation of the vehicle with respect to the sun for portions of long term missions. The absorption cycle potentially provides the needed refrigeration, and could be operated with waste heat as opposed to electrical or shaft power requirements of the vapor compression cycles. This study evaluated the practical requirements of the absorption cycle and the effects of varying operating parameters. No attempt was made to compare relatively the absorption cycle with the vapor compression cycle as previous studies had shown similar potential performance. However, definitive performance data for a spacecraft absorption cycle in zero-g was not available.

The literature was searched to determine the best fluids for a flight-type absorption refrigerator. Fluids were selected on the basis of minimum system weight, minimum radiator area, low power consumption, and safety and operational requirements. Safety requirements alone limited the selection to a small number of fluids. Numerous fluid properties were compared with detailed graphs. The requirement of a large latent heat of vaporization for the refrigerant and a low freezing point narrowed the selection to refrigerants 21, 22, 11, 12, 114 and 216.

The requirements of a high absorbent boiling point and a large absorption capability for the absorbent fluid narrowed the absorbent selection to dimethyl ether of tetraethylene glycol (DME-TEG). The requirement that the refrigerant have a large negative deviation from Raoult's law in the absorbent narrows the refrigerant to R-21 and R-22. For several other fluid properties, R-21, R-22 and DME-TEG were seen to be desirable. From consideration of all properties, the best fluid combination was found to be R-22 and DME-TEG.

Equations were developed which relate pressure, temperature and concentration for a solution of refrigerant and absorbent for R-21 and R-22 in DME-TEG. Enthalpy equations were developed for each fluid as a function of pressure and temperature. Equations defining the heat of mixing associated with mixture of each refrigerant in DME-TEG were also developed.

Refrigeration cycle equations were developed for an idealized absorption refrigeration system with a subcooler and recuperator. The total system was described along with each inherent assumption. No system inefficiencies were considered in the analysis with the exception of an assumed efficiency of 80 percent for the overall performance of the absorber and the generator.

Component weight equations were derived for system radiator components (condenser and absorber), heat exchanges components (recuperator and subcooler) and the system pump. The radiator weights were based on an assumed radiator weight-density and incident heat. Heat exchangers were based on correlations of existing flight exchangers.

Cycle inefficiencies were calculated to provide a measure of the validity of assumptions made in the cycle analysis. Pressure drops, temperature differentials, mass transfer resistances and expansion losses were examined. The results indicated that the system lines, etc., can be sized so that the assumptions made are reasonably valid.

Cycle, fluid and component weight equations were compiled into a computer program for analyzing the refrigeration cycle. Three versions of the program were developed, one nonautomated, one automated on weight minimization and the last automated on radiator area minimization. Programs for R-21 and R-22 were prepared, which were used to conduct parametric analyses for the absorption refrigerator. Results revealed that the case providing a minimum radiator area was R-22 with a generator temperature of 450°F. The penalty for a lower temperature was substantial.

iv

The effects of varying each parameter that was assumed to be at a fixed value were investigated. Each parameter was varied individually while the others were held constant.

From the parametric analyses a test design condition was selected. Safety and stability requirements resulted in the selection of R-22 and DME-TEG with a radiator temperature of 250° F. The program identified all design conditions including temperatures, flow rates, enthalpies, pressures and concentrations at every point in the cycle. Weights and areas were defined as well.

A test system was developed which is based on the test design conditions selected. First, the absorber component was designed, fabricated and tested individually to verify its performance at design conditions. The absorber performed well at equilibrium design conditions. A detailed test procedure is presented which includes steps for cleaning the system prior to being tested. A motion picture, showing the view port at the absorber exit during operation, was prepared and is available.

Next, the generator, separator and recuperator components were designed, fabricated and installed with the absorber for closed loop testing of the total absorbent flow loop. (The condenser and evaporator were simulated with a cooler.) The total system was scaled to 1/53 of the total 35 kW system. Detailed analyses used in determining the component designs are presented, as well as detailed test procedures.

Each component in the total generator-absorber test system operated as designed. Manual control of the total test system, as dictated by the limited funds available for the study, resulted in instability during total system test. As a result, operation was limited to only several minutes for each test. Detailed test results are presented.

A pump-turbine motor study was conducted. Results indicate that a positive displacement hydraulic motor should be used for pressure reduction in the weak solution line and a throttle valve in the refrigerant line.

Detailed conclusions and recommendations are presented. The general conclusion of the study was that the zero-gravity absorption refrigeration system is feasible for use as an environmental control refrigerating system in space vehicles. Supporting conclusions are detailed. The primary recommendation is that investigations into the zero-g absorption refrigeration system should be continued. Specific recommendations are presented.

CONTENTS

NOMENCLATURE

A	area
c	speed of sound
C_p	specific heat
D	tube diameter
DH_m	heat of mixing
DH_r	heat of reaction
f	friction factor
f	function in Eq. (13)
f_i	fugacity of substance i in solution
f_i^o	fugacity of substance i in pure state
g	acceleration of gravity
h	enthalpy
hi	high pressure (in condenser)
K	an equilibrium constant in Eq. 13
ℓo	low pressure (in evaporator)
M	molecular weight Mach number
$\dot{m}$	mass flow rate
p	pressure
p_i	partial pressure of vapor of substance i above the solution
p_i^o	vapor pressure of substance i
q	heat rate
q_{mix}	heat of mixing
R	universal gas constant
T	temperature
U	overall heat transfer coefficient
V_c	core volume

w	weight
WD	weight density
x	axial position in flow channel
x	concentration
x_i	mole fraction of substance i in solution

Greek

α_i	activity coefficient of substance i
γ	ratio of specific heat
ΔT	temperature difference between fluid and wall
ϵ	emissivity of radiators
η	efficiency
ρ	density
ρ_c	core density
σ	Stephan-Boltzmann constant

Subscripts

a	absorbent
abs	absorber
cond	condenser
e	evaporator
eq	equilibrium
g	generator
Hx	heat exchangers (subcooler and recuperator)
hi	high value
in	incident
ℓ	liquid
ℓo	low value
numbers	as identified on Fig. 20
pump	pump
r	refrigerant
rec	recuperator
sub	subcooler
v	vapor

x

Section 1
INTRODUCTION

The advantages of using a refrigeration system in orbital vehicles to provide low temperatures are well known. Basically, refrigeration enables a substantial reduction in the size of radiators required to dump waste ECS heat. The absorption refrigerator has the advantage over the standard vapor compression refrigerator that it can operate on thermal energy rather than shaft energy as required by the latter. This thermal energy is often available at no expense in space vehicles since high temperature waste heat from thermal power sources is dumped overboard.

Absorption refrigeration is now used extensively for earth-bound refrigeration and air conditioning systems. In such systems, the absorption, desorption and liquid/gas separation processes rely heavily on gravity. Furthermore, commercial systems do not always make full use of the potential available in the cycle. Use of such a system in orbital applications requires that the components which normally depend on gravity be operable in both 1 g and neutral or greatly reduced gravity. The accomplishment of this requires the development of capabilities which do not currently exist. Numerous concepts for neutral g operation of the various components of an absorption refrigeration have been proposed. However, with the exception of tests conducted on a zero gravity operable wick-type liquid/vapor separator, none of the concepts proposed have been fabricated and tested. The next step in the natural progression of developing flight hardware is the design, fabrication and testing of a ground refrigeration system which is designed for operation in neutral gravity conditions. This document presents Lockheed's work toward accomplishing that goal.

Section 2

REFRIGERANT-ABSORBENT FLUID PROPERTY DATA

2.1   FLUID LITERATURE SURVEY

Fluids to be used in refrigeration and cooling units for manned space flight applications must fulfill a number of requirements. For example, the safety requirements are quite important. The thermodynamic and transport properties of the fluids considered should be such as to yield a low refrigerator weight and low power consumption for the required performance. In addition, certain operational requirements must be satisfied. Since no single fluid exists that meets all the necessary requirements, establishing certain criteria will aid in selecting the fluids that are best suited for the application to absorption cooling systems.

For reasons of crew safety, the fluids should be:

1. Nontoxic,

2. Nonflammable, and present no explosion hazard when they are in contact with air or oxygen.

From the thermodynamic point of view the following properties are most desirable:

3. The refrigerant should have a high latent heat of vaporization at the evaporator temperature. (This will minimize quantity of refrigerant to be circulated.)

4. Refrigerant and absorbent should display a strong mutual affinity indicated by a strong negative deviation from Raoult's law. (This allows a large difference in concentration between generator and absorber, and reduces the amount of absorbent to be circulated. This has an important consequence. The less absorbent used, the smaller the amount of heat input required in the generator, and a minimum heat input is generally desired.)

5. The absorbent should have a relatively low vapor pressure as compared to the refrigerant. (This will permit a clean separation of refrigerant and absorbent in the generator.)

Finally, from the operational point of view, the following requirements should be satisfied.

6. All fluids should be chemically stable and maintain the liquid state within the range of operational temperatures.

7. All fluids and their decomposition products, if any, must be non-corrosive toward the materials used in the system.

8. The fluids should have a low viscosity in order to minimize pressure losses and maximize heat transfer in the system.

9. Pressures, in general, should not deviate extremely from the ambient pressure in order to prevent bleeding and to enhance light-weight construction.

The final choice of the appropriate refrigerant-absorbent combination from among those which best satisfy the requirements outlined above depends on the resulting weight of the refrigeration system for a given set of conditions. As a rule, this selection is a compromise between conflicting desirable properties.

2.1.1 Fluids Comparison

The safety requirements outlined above considerably limit the search for suitable fluids. Table 1 presents a survey of inorganic and halogenated organic refrigerants with respect to flammability, explosion hazard, and toxicity. The hydrocarbons were deliberately excluded because, although relatively nontoxic, they are highly flammable, and all of them present explosion hazards when they are combined with air or oxygen. Fluids which are deficient in any of the criteria applied should thus not be considered. For the same reasons, the lower alcohols, ethers, and amines should be disregarded. Table 1 shows that, if safety is the overriding criterion, further analysis can be restricted to CO_2, N_2O, SF_6 and H_2O among the inorganic substances, and refrigerants 11, 12, 13, 13B1, 14, 22, 23, 114, 115, 216, and

C318 among the halocarbon components. Necessarily, this survey is limited to fluids for which detailed data are available on their thermodynamic and transport properties (Refs. 1, 2 and 3).

The latent heats of vaporization of various refrigerants are compared in Figs. 1 and 2. Figure 1 displays those of water, ammonia and carbon dioxide with those of some typical refrigerants, while vaporization heats of most of the halocarbon refrigerants are shown on a larger scale in Fig. 2.

It becomes immediately clear that water is the best refrigerant from this aspect. Unfortunately, however, its relatively high melting temperature makes it unsuitable for low temperature cooling. Ammonia would be next best but it must be discarded for reasons of safety. Assuming an evaporator temperature between -40 and $40^{\circ}F$, Fig. 2 shows clearly that, among the inorganic substances, carbon dioxide and nitrous oxide deserve consideration. Among the halocarbons, refrigerants 21, 22, 11, 12, 114, and 216 show the largest heat of vaporization; R-21 has the highest, and R-216 the lowest.

Figure 3 shows the solubility characteristics of the best four organic compounds, viz., refrigerants 21, 22, 11, and 12, in a mixture with dimethyl ether of tetraethylene glycol (DME-TEG). Only R-21 and R-22 (Ref. 4) show the desired negative deviation from Raoult's law while R-11 and R-12 (Refs. 4 and 5) display a positive deviation, very strong for R-12 and less for R-11. Hydrogen bonding or lack of hydrogen bonding is considered to be a significant factor in explaining the solubility characteristics noted in these solutions (Ref. 4).

Absorbents other than DME-TEG were investigated by Thieme and Albright (Ref. 6). It was reported that both, N, N-dimethyl formamide and N, N-diethyl formamide are good solvents for refrigerants 21 and 22, in particular as compared to DME-TEG on a weight basis. However, although they perform well, based on solubility considerations, both have relatively

low boiling points, which might cause problems in an absorption cooling system. Vapor pressures of DME-TEG and refrigerants 21 and 22 are compared in Fig. 4, which also shows vapor pressures for water and other "Ansul-Ethers" (Ref. 7). The desirable low vapor pressure of DME-TEG is particularly noteworthy. Note also the large difference in the boiling point between DME-TEG and R-22. Vapor pressures of other refrigerants and water are compared in Fig. 5. It is interesting to compare some of the refrigerants with respect to their heats of evaporation and their vapor pressures. Carbon dioxide and nitrous oxide, for example, have relatively large heats of evaporation, but they also have very high vapor pressures. Their use would therefore necessitate using relatively heavy equipment. This is in contrast to water, which is distinguished by a large heat of vaporization and very low vapor pressures, as seen from Figs. 1 and 5.

The remaining graphs illustrate the fluid properties that affect the operational aspect of absorption refrigeration systems. Figure 6 displays decomposition data for refrigerant 22 at typical generator temperatures when it is in contact with various materials (Ref. 8; when the data indicated decomposition values of less than 0.001%, they were plotted at 0.001%). From these data it appears that, at least for R-22, chemical stability should be of no concern. However, a cautionary remark is in order. Not only is it uncertain how far these data apply to the refrigerant plus absorbent system, but it should also be noted that aluminum is generally the least reactive metal only because it is protected by an oxide film (Ref. 9). The data for R-22 and oil were taken from Spauschus and Doderer (Ref. 10), and refer to a test duration of 28 days only. Figure 7 depicts more analogous data for refrigerants 12, 114, and 115. Decomposition of refrigerant C-318, for example, is less than 0.001% under all circumstances, and more precise data could not be found. In general it can be said that, in the absence of oil but in the presence of metal, the order of increasing stability is as follows: R-114 = R-12 < R-22 < R-115 (Refs. 8 and 9). When a naphthenic oil is included, the order is in general the same, according to Parmelee (Ref. 8). As a general rule it can also be said that the simpler, chemically, a system can be made, the longer its life should be.

2-4

Another property which is important from the operational point of view is the viscosity. Fig. 8 shows the viscosities of various refrigerants and absorbents in the liquid state as compared to water. It can be seen that, at least in the lower temperature range, all the refrigerants are less viscous than water. DME-TEG appears to be somewhat more viscous than water. Note also that among the refrigerants, R-22, has one of the lowest viscosities, placing it ahead of other refrigerants for operational reasons.

The viscosities of various fluids in the vapor state are shown in Fig. 9. While the viscosity of liquids decreases with increasing temperature, the opposite trend is observed for the vapor state. Also, the viscosities of the vapors are not only about an order of magnitude smaller than those of the liquids, but their spread is quite a bit less.

2.1.2 Conclusions and Recommendations

A large number of fluids for which detailed data could be found in the literature have been surveyed as to their suitability for absorption refrigeration systems to be used in manned space flight. Emphasis was placed on safety, thermodynamic properties and operational criteria. It appears that, among the refrigerants, R-22 is one of the best suited, if not the best overall. It has a relatively high latent heat of vaporization, its vapor pressure is relatively moderate, it is nonflammable, nontoxic and nonexplosive, its chemical stability is very good, and its viscosity in the liquid state is very low compared to other refrigerants. Furthermore, and most important, it displays excellent solubility with DME-TEG. This conclusion, arrived at by a more or less qualitative comparison of the various fluid characteristics is supported by Eiseman (Ref. 12). Among the absorbents which were discussed, DME-TEG was found to be the best for R-22 (Refs. 6 and 4).

With regard to other fluid systems, for which no detailed data could be found, the trends shown in the figures present some recommendations. Both refrigerants 114 and 216 have a relatively large latent heat of vaporization at a relatively low vapor pressure. Their solubility characteristics in

DME-TEG are therefore of definite interest. The same argument holds for water, which is reported to be miscible with DME-TEG (Ref. 7), although it might present problems because of its relatively high freezing temperature.

2.2 FLUID THERMODYNAMIC PROPERTIES DEVELOPMENT

When the various requirements for chemicals to be used in absorption refrigeration systems are considered, especially from the standpoint of performance of such systems, the solubility characteristics of the refrigerant fluid in the solvent fluid are of primary importance (Ref. 4). It is particularly desirable that the refrigerant-absorbent mixture exhibit a large negative deviation from Raoult's law, meaning that the amount of refrigerant absorbed is larger than that predicted for ideal solutions.[*] Therefore, for a given refrigerant flow rate, the absorbent flow rate is smaller, necessitating less heating in the generator and less heat rejection in the absorber. The heat of mixing which generally accompanies high solubility, and its qualitative and quantitative effect on the heat balance is discussed in Section 2.3.

Although the theory of thermodynamics (Refs. 13 and 14) provides the framework, the evaluation of actual functional relationships between pressure, temperature and composition must largely rely on experimental data. However, the analytical description of the solubility characteristics is important for extending or extrapolating experimental data which are normally available only for a limited set of conditions.

The thermodynamic property used to characterize deviations of solutions from the ideal behavior (Raoult's law) is the activity coefficient defined as

$$\alpha_i = \frac{f_i}{f_i^o \, x_i} \tag{1}$$

where f_i and f_i^o are the fugacity of the solute i in solution and the pure solute, respectively; x_i is the mole fraction of the substance i in solution. For

---

[*]A verification of this is presented on page 6-2.

conditions under which the perfect gas law holds, the fugacity may be regarded as the partial pressure, thus

$$\alpha_i = \frac{p_i}{p_i^o \, x_i} \tag{2}$$

Here p_i^o is the vapor pressure of the pure solute i. It can be shown that the activity coefficients should satisfy the Gibbs-Duhem equation, which, for a binary system, reduces to

$$x_1 \left(\frac{\partial \ln \alpha_1}{\partial x_1} \right)_{T,p} = x_2 \left(\frac{\partial \ln \alpha_2}{\partial x_2} \right)_{T,p} \tag{3}$$

where the subscripts indicate the variables to be considered constant.

Analytical solutions to the Gibbs-Duhem equation are known under the names of VanLaar, Margules, and Scatchard-Hamer, among others. The Margules equations, being relatively easy to evaluate, represent a truncated series solution to the Gibbs-Duhem equation, and can be written as

$$\log \alpha_1 = A x_2^3 + B x_2^3$$
$$\log \alpha_2 = A' x_1^3 + B' x_2^2 \tag{4}$$

For a binary system $x_2 = 1 - x_1$, and we can write

$$\log \alpha_1 = A(1 - x_1)^3 + B(1 - x_1)^2 \tag{5}$$

Here A and B are constants under the assumptions stated previously (perfect gas law; constant temperature). In general, however, they must be regarded as functions of temperature. Conditions under which the behavior of the vapors depart appreciably from those of perfect gases impose further limitations on the validity of Eqs. (3) through (5). For cases in which the change of activity coefficient with temperature is unknown or too difficult to evaluate, Colburn and Schoenborn (Ref. 15) stated that some organic

systems follow the approximate rule

$$T \log \alpha_1 = \text{const.} \tag{6}$$

for constant composition.

The present investigation, making use of the above suggestion, shows that the temperature dependence of A and B in Eq. (5) can be evaluated, in an approximate fashion, by fitting a plot of

$$\frac{T \log \alpha_1}{(1 - x_1)^2} = f(1 - x_1) \tag{7}$$

Figures 10 and 11 show such plots for two fluid systems. They were prepared by using experimental data for systems of refrigerants 22 and 21 and dimethyl ether of tetraethylene glycol (DME-TEG), as given by Mastrangelo (Ref. 16). It can be seen that, except for the highest temperatures, the data points follow approximately straight lines. Curve fitting results in the following expressions:

R-22 and DME-TEG:

$$p(x, T) = x \exp\left\{\frac{4720 (1 - x)^3 - 4970 (1 - x)^2}{T}\right\} + \ln p^o \tag{8a}$$

R-21 and DME-TEG:

$$p(x, T) = x \exp \frac{5340 \left[(1 - x)^3 - (1 - x)^2\right]}{T} + \ln p^o \tag{8b}$$

$$\left(T \left[{}^\circ R\right], \ p \left[\text{psia}\right]\right)$$

2-8

The preceding equations agree with those given by Blutt and Sadek (Ref. 17). The vapor pressure term on the right hand sides of these equations is easily evaluated by fitting a curve to a plot of $\ln p^o$ versus reciprocal temperature (see Figs. 12 and 13), resulting in the following expressions:

R-22:

$$\ln p^o = 12.531 - 3.676 \cdot 10^3 \frac{1}{T} - 0.187 \cdot 10^6 \left(\frac{1}{T}\right)^2 \tag{9a}$$

R-21:

$$\ln p^o = 11.983 - 3.860 \cdot 10^3 \frac{1}{T} - 0.439 \cdot 10^6 \left(\frac{1}{T}\right)^2 \tag{9b}$$

$$T\left[^o R\right], \quad p\left[psia\right]$$

For the cycle analysis one is actually more interested in computing the composition as a function of given pressure and temperature. For this purpose it was assumed that x can be represented as a linear function of the logarithm of the pressure p, with temperature T as parameter. The following relations were obtained:

R-22 and DME-TEG:

$$x(p, T) = a(T) + 0.54 \log p \tag{10a}$$

$$a(T) = 3.0 - 0.828 \cdot 10^{-2} T + 0.0413 \cdot 10^{-4} T^2 \tag{10b}$$

R-21 and DME-TEG:

$$x(p, T) = b(T) + 0.53 \log p \tag{10c}$$

$$b(T) = 5.905 - 1.59 \cdot 10^{-2} T + 0.0978 \cdot 10^{-4} T^2 \tag{10d}$$

A comparison of Eqs. (8) and (10), together with experimental data is presented in Figs. 14 and 15. It can be seen that Eqs. (10a) and (10c) adequately represent the experimental data. These equations were used in regions lying outside the range of experimental data.

In addition to the p - T - x relations discussed above, a cycle analysis requires expressions for the enthalpies of the liquids and vapors involved. Curve fitting data from tables and charts (Ref. 3), the following expressions were derived for the enthalpies of saturated liquids (see Figs. 16 and 17):

R-22:

$$h(T) = 0.198 (T - 420) + 18.3 \cdot 10^{-4} (T - 420)^2 - 14.7 \cdot 10^{-6} (T - 420)^3$$

$$+ 4.13 \cdot 10^{-8} (T - 420)^4 \tag{11a}$$

R-21:

$$h(T) = 0.1814 (T - 420) + 9.76 \cdot 10^{-4} (T - 420)^2 - 4.72 \cdot 10^{-6} (T - 420)^3$$

$$+ 0.805 \cdot 10^{-8} (T - 420)^4 \tag{11b}$$

$$\left(T \left[{}^\circ R\right], \ h \left[Btu/lb\right]\right)$$

Expressions for the enthalpies of saturated and superheated vapor can also be obtained by curve fitting pressure-enthalpy charts. This results in the following expressions:

R-22:

$$h(p, T) = 0.1542 (T - 420) + 101.5 - 0.1 \ p\left(\frac{T}{420}\right)^{-2.67} \tag{12a}$$

R-21:

$$h(p, T) = 0.147 (T - 420) + 114.6 - 0.1 \ p\left(\frac{T}{420}\right)^{-1.64} \tag{12b}$$

$$\left(T\left[{}^\circ R\right], \ p\left[psia\right], \ h\left[Btu/lb\right]\right)$$

2-10

These equations are reasonably accurate for moderate pressures. They do not apply for pressures higher than the critical pressures.

Figures 16 and 17 also show saturated liquid enthalpies which result when constant heat capacities are assumed, and these are the enthalpies actually used in the cycle analysis. The need for this simplification arose when it was found that certain optimum temperatures, subcritical for the mixture, are in the supercritical range for the refrigerant (i.e., the critical temperature of the mixture is higher than that of the pure refrigerant). Since, at supercritical temperatures, the concept of saturated liquid becomes meaningless, just as the heat of vaporization, it was assumed that the enthalpy of the liquid refrigerant in the mixture at its temperature could be calculated by assuming a constant heat capacity. For reasons of consistency, this approach was then taken throughout the cycle analysis. A method by Hildebrand and Scott of extrapolating the heat of vaporization above the critical point was examined; however, the C_p extrapolation was more straightforward and was considered just as valid.

2.3   HEAT OF MIXING OF R-21 AND R-22 IN DME-TEG

In contrast to the behavior of ideal gases, it is well known that in the adiabatic mixing of two or more liquids of the same temperature, usually either a temperature increase or decrease occurs. These phenomena can be clearly followed through the introduction of the concept of "heat of mixing."

It is observed that in particular those fluid combinations which exhibit a strong mutual affinity, documented by high solubility and large negative deviations from Raoult's law, also have large heats of mixing. There does not seem to be any method available to determine this heat of mixing purely by analytical means. Instead experimental data must be used. The lack of adequate data considerably hinders the search for an application of new absorbent-refrigerant combinations. Mastrangelo (Refs. 16 and 18) gives equations and solubility data from experiments which, when combined can be used to calculate the heats of mixing for selected organic refrigerants in a mixture with DME-TEG.

2-11

Accordingly, the heat of mixing, ΔH_m, can be calculated from

$$\Delta H_m = \Delta H_r \left(\frac{fK}{1+K}\right) \frac{x_r x_s}{x_r + f x_s - \overline{Z}} \tag{13}$$

where

$$\Delta H_r \doteq -R \left[\frac{d \ln K}{d(1/T)}\right]_f \tag{14}$$

$$\overline{Z} = \frac{\Delta H_m}{\Delta H_r} \tag{15}$$

Here ΔH_m is the heat of mixing per mole solution, ΔH_r is a heat of reaction, R is the universal gas constant, f a function depending on the refrigerant, and K is an equilibrium constant. The terms x_r and x_s are the mole fractions of the refrigerant and the solvent, respectively, in the solution.

Three equations are given by Mastrangelo (Ref. 18) to determine the equilibrium constant K in terms of additional constants K_1 and K_2:

$$K_1 = \frac{1}{f(1+K)} \tag{16}$$

$$K_2 = 1 + \frac{K-1}{f(1+K)} = \frac{f+1}{f} - 2 K_1 \tag{17}$$

Using these equations, K can be expressed in terms of $K_1 = K_1(T)$ for which values are given as a function of temperature:

$$K = \frac{1}{K_1} \frac{f+1}{f} - 1 - K_1 \tag{18}$$

The bracketed term in Eq. (14) can then be evaluated for various refrigerants by plotting $\ln K$ versus $1/T$ ($T^{\circ}K$) (see Fig. 18). Straight lines were assumed to represent an adequate fit to the data. This essentially makes ΔH_r independent of temperature. After ΔH_r is known, the heat of mixing is obtained

2-12

from Eq. (13) by successive approximations until $\overline{Z}$ remains constant. Five to six iterations were found to be usually sufficient to realize a constant value for $\overline{Z}$.

Typical results are shown in Fig. 19 for refrigerant 21 and DME-TEG. Results of present calculations are compared with those of Mastrangelo, and also with experimental results of Zellhoefer and Copley (Ref. 19). The agreement is considered satisfactory. From Fig. 19 it can be seen that approximately 1150 calories of heat are liberated when one-half mole of each, R-21 and DME-TEG, are mixed to give one mole of solution. On a mole basis, this corresponds roughly to 40% of the heat of vaporization of the refrigerant at typical absorber temperatures. In the cycle analysis, however, concentration alternates between the absorber value and the generator value such that the total change in ΔH_m is that between two intermediate values of concentration. Thus, it is concluded that in certain cases the influence of the heat of mixing on the overall heat balance of the cycle may in fact be small; however, depending on the two concentrations it can approach 40%.

The heat-of-mixing equations were incorporated in the cycle analyses discussed in Sections 3 to 5. The actual effect of heat of mixing, as revealed by the computer analysis, was an approximate 10 to 15% increase in generator and absorber weights and the absorber area.

Section 3

ABSORPTION REFRIGERATION CYCLE ANALYSIS

Analysis of the theoretical performance of an absorption refrigeration system is ideally suited to digital computer solution. Equations can be defined which represent the theoretical performance. These equations are categorized for convenience into the following groups:

- Fluid property
- Cycle (mass and heat balance)
- Component weight
- Cycle inefficiencies.

The fluid property equations are discussed in Section 2 along with the fluid literature search. The other three are presented in the following subsections.

3.1 REFRIGERATOR CYCLE EQUATIONS

3.1.1 Discussion

The zero-g absorption refrigerator is shown schematically in Fig. 20. The system consists of two fluid loops. The outer loop (1,2,3,9,4,5,10,6,8 12) can be termed the refrigerant loop. The pure refrigerant portion is shown on a refrigerant pressure-enthalpy chart in Fig. 21. The condenser, subcooler, turbine (or throttle), and evaporator portion of the refrigerant loop is identical to that of a vapor compression cycle. The difference in the vapor compression and the absorption systems is in the method of getting the low pressure refrigerant vapor back to a high pressure vapor to enter the condenser. In the vapor compression cycle, the vapor is compressed, requiring considerable mechanical energy. In the absorption system the vapor is absorbed

3-1

into a liquid absorbent, compressed in liquid form and then desorbed at the high pressure to enter the condenser as a high pressure vapor. By compressing a liquid, far less mechanical energy is required.

The inner loop (3, 9, 4, 5, 11, 7, 13) is the absorbent loop. The absorbent is a liquid which absorbs varying amounts of the refrigerant depending on the pressure and temperature of the solution. In the generator the pressure and temperature are such that refrigerant vapor is evolved from the solution. Therefore, since the refrigerant vapor is taken out at the separator, a weak solution exists through 11, 7, 13. The weak solution, throttled or expanded to a new pressure and temperature, absorbs the refrigerant returning from the subcooler. The pump provides the pressure increase for the rich solution leg (3, 9, 4, 5).

Turbines can be considered for pressure reduction devices instead of throttle valves. The gain is twofold: the turbine energy is used to power the pump, and the enthalpy level of the refrigerant entering the absorber is reduced.

The recuperator and subcooler are used to increase the overall system efficiency.

Heat added in the generator provides the heat of vaporization (and heat of mixing) to evolve the vapor. Heat rejected from the absorber removes the heat of vaporization (and mixing) to absorb the vapor in the liquid.

3.1.2 Equations Development

The equations which describe the cycle performance are presented in the following paragraphs. Maximum utilization was made of previous work in this area (Ref. 17).

The refrigeration capacity, q_e, is assumed known. It is assumed there is no absorbent in the refrigeration loop. The expansion processor are

3-2

assumed isenthalpic. It is assumed that only heat of vaporization is added to the fluid at the evaporator. Therefore, the liquid flow rate into the evaporator is:

$$\dot{m}_{\ell, e} = \frac{q_e}{h_{v, 1} - h_{\ell, 1}}$$

Some refrigerant enters the evaporator as saturated vapor. This is because the subcooling is not sufficient to prevent some vaporization in the refrigerant turbine. Therefore,

$$\dot{m}_{v, e} = \dot{m}_{\ell, e} \left(\frac{h_8 - h_\ell}{h_v - h_8} \right)$$

where $$h_8 = h_6 - h_2 + h_1,$$

obtained from a heat balance on the subcooler. The numeric subscripts refer to locations shown in Fig. 20.

Equilibrium concentrations of the solution in the absorber and the generator, XAE and XAG, respectively, are obtained by fluid property equations presented in Section 2. The refrigerant concentrations at the absorber and generator exits are derived from the two efficiency equations:

$$\eta_a = \frac{x_{abs} - x_g}{x_{abs, eq} - x_g}$$

$$\eta_g = \frac{x_{abs} - x_g}{x_{abs} - x_{g, eq}}$$

The basis for these efficiency equations is presented in Section 3.3.3.

3-3

The resulting concentrations are:

$$
x_{abs} = \frac{\eta_g x_{g,eq} + \dfrac{\eta_{abs} + x_{a,eq}}{1 - \eta_{abs}}}{\eta_g + \dfrac{\eta_{abs}}{1 - \eta_{abs}}}
$$

$$
x_g = \frac{\eta_{abs} x_{abs,eq} + \dfrac{\eta_g x_{g,eq}}{1 - \eta_g}}{\eta_{abs} + \dfrac{\eta_g}{1 - \eta_g}}
$$

The refrigerant flow rate in the weak solution and the total absorbent flow rate are now derivable from quantities already defined.

$$
\dot{m}_{r,11} = \frac{\left(\dot{m}_{\ell,e} + \dot{m}_{v,e}\right)\left(1 - x_a\right) x_g}{x_a - x_g}
$$

$$
\dot{m}_a = \frac{M_a \dot{m}_{r,11} \left(1 - x_g\right)}{M_r x_g}
$$

The energy exchange in the recuperator is evaluated in the weak solution leg:

$$
q_{rec} = \dot{m}_{r,11}\left(h_{r,5} - h_{r,7}\right) + \dot{m}_a\left(h_{a,5} - h_{a,7}\right)
$$

The enthalpy at point 4 is now obtainable:

$$
h_{a,4} = h_{a,3} + \frac{q_{rec} - \left[\dot{m}_{r,3}\left(h_{r,4} - h_{r,3}\right)\right]}{\dot{m}_a}
$$

3-4

The heat loads at the absorber, condenser subcooler, and generator are now determined:

$$q_{rec} = \dot{m}_{r,11} \left(h_{r,5} - h_{r,7} \right) + \dot{m}_a \left(h_{a,5} - h_{a,7} \right)$$

The enthalpy at point 4 is now obtainable:

$$h_{a,r} = h_{a,3} + \frac{q_{rec} - \left[\dot{m}_{r,3} \left(h_{r,4} - h_{r,3} \right) \right]}{\dot{m}_a}$$

The heat loads at the absorber, condenser subcooler, and generator are now determined:

$$q_{abs} = \dot{m}_{r,1} h_2 + \dot{m}_{r,11} h_{r,7} - \dot{m}_{r,3} h_{r,3} + \dot{m}_a \left(h_{a,7} - h_{a,3} \right)$$

$$+ q_{mix,3} - q_{mix,7}$$

$$q_{cond} = \dot{m}_1 \left(h_{r,5} - h_6 \right)$$

$$q_{sub} = \dot{m}_1 \left(h_2 - h_1 \right)$$

$$q_{gen} = \dot{m}_1 h_{r,v,5} + \dot{m}_{r,11} h_{r,\ell,5} - \dot{m}_{r,4} h_{r,4}$$

$$+ \dot{m}_a \left(h_{a,5} - h_{a,4} \right) + q_{mix,4} - q_{mix,5}$$

The pump power requirement is calculated as follows:

$$q_{pump} = \left[\frac{\dot{m}_{r,3}}{\rho_r} + \frac{\dot{m}_a}{\rho_a} \right] 0.185 \left(P_{hi} - P_{\ell o} \right)$$

3-5

where the coefficient is the conversion from flow energy to heat energy.

These cycle equations are used in the computer program presented in Section 3.4.

3.2 COMPONENT WEIGHT AND RADIATOR AREA EQUATIONS

In the design of an absorption refrigeration system it is desirable to minimize two system parameters: the total system weight, and the total radiator area. These two parameters are almost proportional to each other since the radiators constitute the bulk of the total weight. However, when large demands are made of other system components, their weights can rise rapidly. For example, as the absorbent flow rate rises, the recuperator and generator weights increase. Also, when increased efficiency requirements are placed upon the subcooler and the recuperator their weights increase accordingly. Therefore, it is desirable to treat both area and weight in the parametric evaluations.

A radiator area requirement is easily obtained, a simple and definite function of the radiator temperature, the required net heat flux from the radiator and the incident heat to the radiator.

Weight is far less well defined. The weight density of a radiator is variable. Furthermore, the weights of other components depend on flow rate, heat rate and component efficiency and these dependencies are not clearly defined. Therefore, the safest approach is to simply optimize the total radiator area. The radiator area equations are simply:

$$A_{abs} = \frac{q_{abs}}{\sigma \epsilon \, T_{abs}^4 - q_{in}}$$

$$A_{cond} = \frac{q_{cond}}{\sigma \epsilon \, T_{cond}^4 - q_{in}}$$

However, in order to deal at all with total system weights, equations must be defined that relate the component weights to performance. The weight of the two radiator components (absorber and condenser) are assumed to be:

$$w_{abs} = \frac{(WD) \, A_{abs}}{2}$$

$$w_{cond} = \frac{(WD) \, A_{cond}}{2}$$

The terms WD and q_{in} will be varied in the parametric analysis so that the influence of each parameter is identified.

The equation for the pump assembly was determined by plotting weight versus hydraulic horsepower for several pump modules that are currently being used for space application. An equation was then written for this curve. The resulting equation for the pump assembly weight was given by:

$$w_{pump} = 0.546 \left[\frac{8.72 \, \dot{m}_3 \left(P_{hi} - P_{\ell o} \right)}{\rho} \right]$$

where

$$\rho = \frac{\dot{m}_3}{\dfrac{\dot{m}_a}{\rho_a} + \dfrac{\dot{m}_{r,3}}{\rho_r}}$$

This pump assembly weight equation agrees quite well with other pump weight equations given in various reports when the weight of the driving motor and required gears are added to the pump weight.

An extensive literature survey was conducted to obtain a reasonable weight equation for heat exchangers (recuperator, subcooler) as a function

3-7

of their performance. The best information found was from Shaffer (Ref. 20)
The equation obtained that relates performance to heat exchanger weight is

$$w_{Hx} = 1.475 \; \rho_c \; V_c^{0.882} \quad,$$

where ρ_c is the core density and V_c is the core volume. The core volume
is calculated by

$$V_c = \frac{q}{U\bar{A}\,\Delta T} \quad (ft^3)$$

where $\bar{A} = (A/V_c) \sim ft^2/ft^3$ and is called the surface area density and ΔT in
our case is the log mean temperature difference (LMTD) for the heat
exchanger.

The values of core density and core surface area density as given by
Shaffer for various type heat exchangers are:

Type of Surface		Core Weight Density, lb per ft³ of Core Vol.	Surface Area Density, ft² per ft³ of Core Vol.		Applications
			Side 1	Side 2	
Plate-Fin	Al	31.1	131	359	Liquid to gas. Moderate-pressure gas to low-pressure gas.
	SS - Ni	69.8	140	375	
Tubular	Al	18.1	143	155	Gas to gas.
		32.0	203	231	
	SS	33.1	166	166	
Finned Tube	Al	19.2	46.7	597	Liquid to gas. High-pressure liquid or gas to low-pressure gas.
	SS				
Shell and Tube	Al	34.1	280	313	Liquid to liquid.
	SS	62.4	293	313	

Since Shaffer is a staff member of Airesearch Manufacturing Company who provides compact heat exchangers for space applications, it was felt that his equation and data for heat exchangers were probably the best available and were therefore used in this study.

3.3 CYCLE INEFFICIENCY EQUATIONS

The computer program as currently in operation assumes an idealized cycle performance, i.e., with no inefficiencies. (The only exception is that a quantitative inefficiency can be assumed and input for the mixing and separation process in the absorber and generator, respectively. However, no experimental or analytical data are used to justify the assumed values.) A number of inefficiencies warrant consideration. These are the:

1. Pressure drop in flow lines
2. Driving temperature potential required in each heat transfer device
3. Mass transfer resistance associated with absorbing and desorbing the refrigerant in the absorbent
4. Inefficiency in the expansion throttle valves.

There is no question that these factors degrade the system performance. The question is the extent. Quantitative definition depends on a physical description of the components of the refrigerator. Some degradation factors may be such that they are insignificant regardless of the component configuration. Others may be appreciable.

These five inefficiencies are discussed in the following sections:

3.3.1 Pressure Drop Losses

Calculations were performed to determine the pressure loss at each section in the refrigeration cycle. The flow conditions used in the calculations were those selected as design values in the parametric analyses of Section 4.

These flow conditions are presented in Table 2. The results of these calculations for numbered points in the cycle (Fig. 20) and for the condenser and the absorber are presented in Figs. 22 and 23. The pressure gradient is shown for each flow position as a function of the flow line diameter. These results reveal that the flow channels can be sized so that pressure losses are reduced to insignificant values.

3.3.2 Driving Temperature Required to Each Heat Transfer Device

A finite temperature difference exists between the condensing fluid in the condenser tubes and the radiating surface of the condenser. This ΔT, ignored in the computer solution, is inherent in the absorber, evaporator and generator as well. This means, in the condenser for example, if the refrigerant condensation is taken to occur at some temperature, T_{cond} (value used in the computer analysis), the radiating surface of the condenser will be at $T_{cond} - \Delta T$. This inefficiency or loss could easily be treated in the computer solution if it were known. However, its actual value is dependent on the exact design of the condenser which is not presently known. Therefore, in order not to introduce an unknown into the computer solution, the ΔT in the several components is treated as zero. For the purpose of the computer solution it is adequate to be aware of the assumption being made and to have a feel for the range of values that can exist for ΔT, and the effect on each component.

In the generator, ΔT is not critical since the heat source temperature can be higher than the fluid temperature in the generator without a penalty. In the condenser and the absorber ΔT is important because it results in a direct penalty (reduction) in the radiator temperature. The absorber ΔT is assumed to behave quite similar to the condenser ΔT since in both a vapor is being converted to a liquid. The evaporator ΔT is important also because it causes a direct penalty in the refrigerating temperature. That is, if the refrigerant evaporation is taken to occur at T_e (value used in computer

3-10

analysis), the evaporator tube walls will be at $T_e + \Delta T$ and the fluid being refrigerated (air, for environmental control) will be at $T_e + \Delta T + \Delta T'$. For these reasons, calculations were conducted to define these temperature differentials for the condenser and the evaporator. Curves of film coefficients and ΔT versus tube diameter for the condenser and the evaporator are presented in Figs. 24 and 25, respectively. Clearly, the tubes can be sized to minimize the temperature differential inefficiency.

3.3.3   Mass Transfer Resistance in Absorber and Generator

In the absorber and the generator, one fluid, the refrigerant, is being absorbed or desorbed, respectively, by a second fluid, the absorbent. There- fore, mass transport of one liquid within the other becomes a potential rate constraint. For example in the absorber, the refrigerant gas is "condensing" on the surface of the absorbent solution which is weak in refrigerant. Unless this newly absorbed refrigerant is somehow removed from the surface of the solution, the solution at that point will become saturated with refrigerant and absorption will cease. (Just the opposite process applies for the generator.) It is important to understand what happens when this saturation occurs. If the absorber temperature remains constant following this saturation, absorp- tion ceases. However, this is not expected to be the case. Heat is being removed from the absorber due to the release of heat of vaporization and heat of mixing. Since this heat removal from the solution is being maintained by the external conditions (i.e., radiation from the tubes via fins for a space radiator) it is not likely to stop when absorption stops. This heat removal continues and instead of being balanced by vaporization the fluid temperature drops. This temperature drop is undesirable in the absorber and can be prevented only by adequate mass transfer. (The corresponding effect in the generator is a temperature rise caused by heat addition with desorption.)

Removal of the newly absorbed refrigerant from the solution surface is accomplished by mass diffusion or by physical mixing as caused by turbulence. In order to examine this potential problem, a model must be

assumed. The model for the absorber is essentially prescribed by the physical constraints. A finned tube condensing radiator must be assumed. The liquid solution is assumed to be a film on the tube wall surrounding a refrigerant vapor core.

Calculations reveal that the liquid film is turbulent. A careful literature search did not produce a solution to the problem of mass transfer of a single component vapor into a turbulent binary liquid film. Even an attempt to treat the problem as laminar with pure diffusion was unsuccessful as no diffusion coefficient data was available for R-22 in DME-TEG. With these obstacles to a direct solution to the mass transfer problem, an intuitive approach was taken. A direct comparison between the mass transfer and the heat transfer in the absorber was made. Upon first examination, the heat and mass transfer are quite analogous in the absorber. Heat and mass must be transferred from the vapor core into the liquid film. This part is analogous. However, going a step further the analogy fails. The heat must now pass through the liquid film, into the tube wall, through the fin and then radiate to space. The mass transfer stops when the absorbed vapor, now a liquid is passed from the film surface into the film. In turbulent flow this difference is substantial. Heat must pass through a laminar liquid sublayer adjacent to the tube wall to get to the tube. Obviously, this sublayer is far more resistant to transport than the turbulent portion of the film, not to mention the remaining resistances in the heat flow path. It becomes quite clear that with turbulent flow the heat transfer would be expected to be the controlling mechanism. (This fact had been anticipated before the transport analysis was done. The turbulence of the liquid film was thought to be adequate to maintain fresh, non-equilibrium liquid at the film surface.) The heat transfer analysis of the absorber is considered to be similar to that of the condenser which is treated in Section 3.3.2.

The next step was to evaluate this intuitive analysis experimentally. This was performed and is documented in Section 6 of this report. As discussed there, the absorber performed as designed.

3-12

The preceeding analysis related to the ability of the weak solution to absorb the refrigent vapor by turbulence. This absorption can occur, however, only when the solution is "weak" or below its equilibrium value in refrigerant. As absorption proceeds down the tube and the solution approaches equilibrium, the absorption rate is retarded by the reduced driving differential. A point is reached where, even with the turbulence discussed previously, the absorbtion rate reduction results in a temperature decrease of the radiator. To prevent this, it will be assumed that the solution will exit the absorber at some concentration below equilibrium. The efficiency of the absorber will, therefore, be defined as:

$$\eta_{abs} = \frac{x_{abs} - x_g}{x_{abs,eq} - x_g}$$

A similar equation for the generator is presented in Section 3.1. For the purposes of this study the absorber and generator efficiencies will be set at 80%. The effect of varying this percentage is presented in Section 4.

3.3.4   Expansion Losses

The enthalpy rise in the strong solution pump and the enthalpy drop in the weak solution and refrigerant expanders are each less than 1 Btu/lb_m which is negligible in the total system.

Losses in the expanders can therefore be ignored. The important aspects of the expanders are their potential to: (1) establish a pressure differential (throttle valve) between P_{hi} and P_{lo}; (2) meter the flow (positive displacement hydrolic meter) through the refrigerant and/or weak solutions lines; and (3) provide power to reduce the electrical power requirement of the pump. These are discussed at length in Section 8 which deals with the pump-turbine-motor package.

3.4 COMPUTER PROGRAM DEVELOPMENT AND AUTOMATION

Equations derived and selected to define the performance of a zero-g absorption refrigeration system were presented in Sections 3.1 and 3.2. Assumptions regarding line and component pressure losses and temperature differentials between fluids and components were justified in Section 3.3.

The equations were developed into a digital computer program which solves the entire absorption cycle based on the assumptions made. Three versions of the program were developed. The first version (Version 1) requires that the following six temperatures be prescribed and input: evaporator, T_e; generator, T_g; subcooler, T_{sub}; recuperator, T_{rec}; absorber, T_{abs}; and condenser, T_{cond}. This program simply calculates, for these fixed temperatures, the system pressures, enthalpies, flow rates, heat loads, component weights, radiation areas, refrigerant concentrations, etc., around the system.

The basic program described above was modified into two automated versions. These two versions are programmed to automatically minimize the total refrigerator system weight (Version 2) or total system radiator area (Version 3), respectively. By inputting only the generator and evaporator temperatures, the program automatically calculates the remaining component temperatures which correspond to minimum weight or area. Since the optimized temperatures are interdependent, the optimum value of one will vary when the other temperatures are changed. Therefore, a convergence criterion is a key to the optimization scheme. Weight and area optimized versions of each were set up with R-21 and R-22 equations.

For all versions of the program, the following assumptions are made. Most of these assumptions follow directly from Sections 3.1 to 3.3:

1. Pressure changes in the flow line occur only at the pump and the throttle valves (see Fig. 20 and Table 2).

2. Temperature changes occur in the absorber, recuperator, generator, condenser and subcooler. No changes occur in flow lines.

3. The expansion and compression processes are isenthalpic.

4. The radiator area calculations (for absorber and condenser) assume the entire radiator surface is at the component exit temperature. This is conservative since the area would be smaller than calculated.

5. A value of incident heat flux to the radiators must be assumed.

6. A value of radiator weight density (weight per unit area) must be assumed.

7. An overall efficiency for the absorber and the generator must be assumed.

8. Complete separation occurs in the separator.

9. No absorbent enters the condenser.

10. The efficiency of the heat exchangers ($T_7 - T_9$ for the recuperator and $T_8 - T_1$ for the subcooler) are input to Version 1 and Version 3 while they are optimized for Version 2 (weight optimized case).

11. Radiator emissivity = 0.9.

The area optimized version with R-22 equations is presented in Appendix A. Parametric results of the program runs are presented in Section 4.

Section 4
PARAMETRIC CYCLE ANALYSIS

The cycle optimization computer program discussed in Section 3 was used to define the best refrigeration cycle design based on the idealized conditions assumed. A nominal value was selected for each of the several optional parameters to arrive at the following nominal case:

q_{in}:   50 Btu/hr-ft^2 on each side of the radiator

WD: 2 lb$_m$/ft^2

q_e: 35 kW

$\eta_{abs} = \eta_g = 0.8$

$T_e = 40^{\circ}F$

Optimization cases were run for two fluids (R-21 and R-22 with DME-TEG), two different optimization routines (system weight and radiator area minimization) and seven different generator temperatures (200 to 500°F). A composite of all these calculations is shown in Fig. 26. The figure reveals that for the assumptions made, the optimum generator temperature for R-22 is approximately 450°F for a minimum total radiator area and approximately 415°F for a minimum total system weight. For R-21 the same two temperatures are approximately 330°F and approximately 285°F, respectively. Furthermore, it shows that for area optimization, R-22 is superior above 265°F while R-21 is superior below that temperature. For weight optimization, R-22 is superior above 340°F while R-21 is below that temperature. The overall best combination for minimum area is R-22 at T_{gen} = 450°F. The penalty of going to a lower temperature is substantial.

Note that the weights corresponding to optimized areas and the areas corresponding to optimized weights are also presented on Fig. 26.

The total system weight used in the optimization is the combined weight of the absorber, pump, recuperator, condenser, subcooler and the liquid in the recuperator and the subcooler. In the weight optimized run four separate parameters are being optimized as follows:

$$T_3 \quad (T_{cond})$$

$$T_6 \quad (T_{abs})$$

$$T_7 - T_9 \quad \text{(dependent on recuperator efficiency)}$$

$$T_6 - T_2 \quad \text{(dependent on subcooler efficiency)}$$

Weight optimization of $T_7 - T_9$ and $T_6 - T_2$ is possible since the recuperator and subcooler weights go up rapidly as these temperature differences approach zero. A minimum exists at some point. Radiator area does not have such a minimum for these two temperature differences. Therefore, area optimization cannot be done on $T_7 - T_9$ and $T_6 - T_2$. The solution to this problem was to do the weight optimization first and then use the efficiencies therefrom as fixed values in the area optimization. Therefore, the area optimization is done on only T_3 and T_6.

Absorber and condenser temperatures which correspond to optimum conditions for each optimization case conducted are shown in Fig. 27 for R-22 and Fig. 28 for R-21.

Version 1, the non-automatic version of the program was used to observe the effects of varying the absorber and condenser temperatures from their optimum values for the area optimization, R-22 case. The results are shown in Fig. 29. This verifies that the optimization program is correct and it shows the penalty for off design.

All the preceding calculations were for a fixed value of radiator weight density, incident radiator heat flux and generator and absorber efficiencies. Furthermore, the area optimization cases were for fixed subcooler and recuperator efficiencies (based on corresponding results from weight optimization). Since these selections were based on anticipated conditions and were therefore arbitrary, it was considered desirable to show the independent

4-2

influence of each one. This was done using the area optimization program. The results are shown in Figs. 30 through 34. The optimized area and the total system weight are shown as a function of each of these parameters. Each point on each curve is an area optimized value. The nominal value of each parameter is used when another is being varied. The nominal value of generator temperature was assumed to be 250° for one reason — that was the value chosen in Section 5 for testing. Each parameter is seen to influence the total system weight and/or area except $T_6 - T_2$. $T_6 - T_2$ does influence the subcooler weight; however, the subcooler weight is such a small portion of the total system weight that it does not show up appreciably.

A cycle analysis for R-22/DME-TEG was conducted using a zero deviation from Raoult's law. This fictitious situation was run simply to verify, by computer analysis, the stated need for a large deviation from Raoult's law. The case was exactly the same as a standard R-22/DME-TEG except Raoult's law was used in the program in place of the experimental data available on R-22 in DME-TEG. Also, since heat of mixing is due to a deviation from Raoult's law, heat of mixing was eliminated in the fictitious run. The results of this comparison are: At a generator temperature of $250^{\circ}F$, the new case resulted in an increase in total radiator area of from 2541 ft^2 to 2798 ft^2 (10.1%) and an increase in total system weight of from 3605 lb_m to 4213 lb_m (16.9%). These results verify the need for a large deviation from Raoult's law.

Section 5
CYCLE DESIGN

Results from the parametric cycle analyses were used to define design conditions for the experimental phases of the study. The selection was based on using area optimization results rather than weight optimization. This choice was made in consultation with Mr. R.L. Middleton, the NASA Contracting Officer's Representative (COR). The choice is substantiated by the fact that the weight equations used in the program are more susceptible to error than the radiator areas equations and are therefore a more reliable criterion. Actually, most of the system weight is attributed to the radiators for which weight is proportional to area. The non-radiator components are those which have only approximately defined weight equations.

The design condition selected was the minimum area case of Fig. 26 which corresponded to R-22 with a generator temperature of 450°F. However, there is some question about the stability of a solution of R-22 and DME-TEG above 350°F. Furthermore, there was some concern about safety at the extremely high pressure (452.5 psia) associated with a 450° generator temperature. Therefore, in mutual agreement with Mr. Middleton, the generator temperature was set at 250°F. At this generator temperature the high pressure was 248 psia.

It is noteworthy that at $T_g = 250^\circ$F, R-21 is superior to R-22. However, R-22 was retained because it is anticipated that a flight system would be operated at 300 to 350°F such that R-22 would again be superior. It is interesting that the total system weight for R-22 (from Fig. 1) is better at $300 - 350^\circ$F than at 450°F anyway.

The exact flow conditions at each point in the cycle for R-22 and $T_g = 250^\circ$F is shown in Table 2. The numbered locations correspond to those on Fig. 20.

5-1

Section 6
ABSORBER TEST SYSTEM

A preliminary test system to evaluate the absorber component has been designed, fabricated and assembled. All surfaces wetted by the fluids are made of stainless steel. The absorber radiator area for $T_G = 250^\circ F$ is taken to be 608 ft^2 on one side. Assuming a rectangular configuration of 23 ft by 26.5 ft and a 6-inch tube separation, a total of 53 tubes will be used. In the present test, the flow rates are scaled down to 1/53rd and the cooling length of the absorber tube is 23 ft.

6.1 EXPERIMENTAL ARRANGEMENT AND APPARATUS

A detailed flow diagram of the test system is shown in Fig. 35. (Drawing No. A401). The weak solution is drawn from the mix tank where the components have been mixed to yield the given concentration of R-22. The tank has been preheated and pressurized. The weak solution supply line is adjusted to achieve the scaled down flow rate. The R-22 vapor from the preheated containers passes through the immersion heaters before entering the mixing section. Cooling water is admitted to the absorber outer jacket. A view section was installed after the absorber for visual inspection of the exit flow. The inlet and the exit sections of the absorber are shown in Figs. 36 and 37, respectively.

All pressure vessels were tested to satisfy the "Safety and Industrial Hygiene Standards" (C-12) of Lockheed Missiles & Space Company.

For purpose of sizing the test system, tests were conducted to determine the temperature-dependent specific gravity of DME-TEG (Ansul E-181). The details of the tests are given in Appendix B and the absorber design in Appendix C.

6.2   TEST PROCEDURES

A detailed test procedure has been written for the absorber test which includes a discussion of pre-test cleaning steps, safety measures and actual test procedures. An abbreviated version is given in Appendix D.

The absorber test is completed when clear liquid (complete absorption) is observed at the view section while the fluids are maintained at the specific conditions at the absorber inlet.

6.3   TEST RESULTS

The absorber test was completed successfully with weak solution and R-22 vapor introduced into the absorber at design conditions. A strong solution was obtained at the exit with no vapor present. A rerun of the test was made under similar conditions, and motion pictures were taken to show the test apparatus and the flow patterns at the exit of the absorber. The test results and the scenario for the motion picture are given in Tables 3 and 4.

Section 7
ABSORBER AND GENERATOR TEST SYSTEM

7.1 TEST LOOP AND COMPONENTS

A schematic view of the test loop for evaluating the absorber and generator components is shown in Fig. 38 (Drawing No. A402). The loop includes the flow lines, the absorber, the generator, the recuperator, the pump, the separator and the cooler (which represents the condenser and the evaporator for a complete absorption refrigerator). The transfer lines are 0.75-inch o.d. stainless steel tubing with 0.035-inch wall. The details of the final design of the recuperator, generator, separator and the cooler are given in Appendixes E to H. The assembling of various components and the insulated test loop are shown in Figs. 39a to 39h.

The design requirements given in Table 2 scaled to 1/53rd scale were those used as test design conditions.

7.2 TEST PROCEDURES

The test loop is filled with solution of specified R-22 refrigerant concentration from the liquid surge and feed tank. R-22 vapor is either generated in the generator or admitted to the system directly into the absorber. The strong solution from the absorber passes through a pump where the pressure is raised from 84 psia to 248 psia. The temperature of the strong solution is then increased through a recuperator before being heated in the generator. The weak solution from the separator passes through the recuperator and back to the absorber. The R-22 vapor from the separator is cooled in a cooler before being throttled down to the absorber inlet. An outline of the actual test procedure is given in Appendix I.

7-1

7.3   TEST RESULTS

Testing on the closed loop generator-absorber test system verified each system component. Each individual component operated satisfactorily — the absorber, generator, recuperator, separator and cooler. Results indicate that the design of each independent component was more than adequate; however, manual control of the total system, as dictated by the limited funds available for the study, resulted in instability during total system test. For example, a fixed pump speed dictated a bypass valve for flow control. This recycling of the same fluid through the pump caused the fluid to become excessively warm which ultimately led to off-design conditions at best and pump cavitation at worst. These and other instabilities precluded prolonged operation at design conditions.

Results regarding each of the components taken individually are as follows:

Absorber: Complete absorption occurred in the absorber.

Generator: Good vapor generation occurred in this component.

Separator: The separator provided good vapor/gas separation.

Recuperator: The high demand requirement of the recuperator was met.

The actual test conditions during the system tests were those presented in Table 5. As mentioned previously these conditions were sustained only for several minutes.

Recommended design changes are presented in Section 9.

Section 8
PUMP-TURBINE-MOTOR PACKAGE STUDY

A study was conducted to assess the use of turbines in place of throttle valves in an absorption refrigeration system designed to be used in an orbiting space station. There are two throttle valves in a typical absorption refrigerating system which are used to drop the pressure in the weak solution line and the refrigerant line. As the drop in pressure through the throttle valves represents energy loss to the system, the question of energy recovery by the use of turbines or by other means immediately suggests itself when the refrigeration system is considered for space use.

An assessment of the pump-turbine-motor package development requirement was conducted and it was concluded that a pump-turbine-motor package is not the most efficient or desirable way to recover useful energy from the system. To achieve the same results for conditions that exist in the system, a positive displacement hydraulic motor offers higher efficiencies and better control capability over a wide range of loads and speeds. A detailed study on the hydraulic-motor-pump-electric motor package approach is given in Appendix J.

Section 9
CONCLUSIONS AND RECOMMENDATIONS

9.1   CONCLUSIONS

The general conclusion drawn from this study is that the zero gravity absorption refrigeration system is feasible for use as a refrigerating system in spaceflight vehicles. The conceptual development of the refrigeration system verified its applicability. Prototype tests of the absorber and generator substantiated the conceptual design for those components.

Specific conclusions that can be drawn from the study are:

1. The detailed fluids investigation revealed that the combination of R-22 and DME-TEG was the best available for existing refrigerant-absorbent combinations for the application required.

2. The various refrigeration system inefficiencies such as line friction and momentum pressure losses and temperature drops between fluids and line walls can be made negligible by properly sizing the flow lines.

3. The ideal generator design temperature to minimize radiator area is 450°F; however, the initial prototype design condition was 250° to assure stability of the fluids.

4. The absorber prototype performed well at design conditions. The test confirmed the analytical prediction that turbulence in the absorber tube coupled with the strong affinity of the absorbent for the refrigerant produced good absorption.

5. The generator prototype was operated and successfully generated vapor. It was not operated at exact design conditions, however, because of control problems.

6. The recuperator, 1 g separator and cooler operated successfully.

7. The pump-turbine-motor package study requirements reveals that the best means of recovering energy from the expansion process is to use a positive displacement hydraulic motor in the weak solution line. No energy recovery system should be used in the refrigerant line.

9-1

9.2 RECOMMENDATIONS

Based on the successful operation of the several absorption refrigeration components, it is recommended that the study be continued. Specific recommendations for further work are as follows:

1. Conduct a study of the controls required to attain stable operation of the total absorber-generator system and make these determined revisions.

2. Conduct tests on the total system to obtain performance over a range of generator temperatures and over a range of absorber inlet refrigeration concentrations. Obtain test results at several off-design conditions.

3. Using the cycle performance computer program, conduct additional parametric performance analyses which incorporate the following:

    ● Alternate system configurations (i.e., additional heat exchangers).

    ● Modified component weight and radiator area equations based on results obtained in other future work tasks.

    ● A more refined absorber and generator mass transfer model based on future parametric testing of the two components.

    ● Heat transfer and pressure drop inefficiencies in the cycle.

4. Design, analyze, fabricate and experimentally evaluate a zero-g liquid/vapor separator component for the absorption refrigeration system.

5. Conduct detailed design analyses of the condenser, absorber, generator and evaporator. Generate from these studies a detailed flight prototype design for each of the four components.

6. Develop a computer capability for modeling the steady state and transient performance of the absorber and generator. Integrate this into the existing cycle performance computer program and conduct parametric analyses.

7. Conduct systematic investigations to synthesize new refrigerant absorbant combinations which are superior to presently known fluids. Reduce any such fluids to equations for use in the cycle computer program and conduct computer analyses of the fluids.

9-2

Section 10

REFERENCES

1. ASHRAE Guide and Data Book, "Fundamentals and Equipment for 1965 and 1966," New York.

2. Hirschberg, H.G., Kältemittel, Verlag C.F. Müller, Karlsruhe, Germany, 1966.

3. Air Conditioning Refrigerating Data Book, 10th Edition, The American Society of Refrigerating Engineers, 1957.

4. Albright, L.F., T.C. Doody, P.C. Buclez, and C.K. Pluche, "Solubility of Refrigerants 11, 21 and 22 in Organic Solvents Containing an Oxygen Atom," ASHRAE Transactions, Vol.66, 1960, pp.423-433.

5. Hesselberth, J.F., and L.F. Albright, "Solubility of Mixtures of Refrigerants 12 and 22 in Organic Solvents of Low Volatility," ASHRAE Transactions, Vol.71, 1965, pp.27-33.

6. Thieme, A., and L.F. Albright, "Solubility of Refrigerants 11, 21, and 22 in Organic Solvents Containing a Nitrogen Atom and in Mixtures of Liquids," ASHRAE Transactions, Vol.67, 1961, pp.431-441.

7. "Ansul Ethers," The Ansul Company, Marinette, Wisconsin.

8. Parmelee, H.M., "Sealed-Tube Stability Tests on Refrigeration Materials," ASHRAE Transactions, Vol.71, Part I, 1965, pp.154-161.

9. Eiseman, B.J., "Reactions of Chloroflurorohydrocarbons with Metals," ASHRAE Transactions, Vol.69, 1963, pp.371-379.

10. Spauschus, H.O., and G.C. Doderer, "Chemical Reactions of Refrigerant 22," ASHRAE Transactions, Vol.71, Part I, 1965, pp.162-168.

11. Witzell, O.W., and J.W. Johnson, "The Viscosities of Liquid and Vapor Refrigerants," ASHRAE Transactions, Vol.71, Part I, 1965, pp.30-35.

12. Eiseman, B.J., "Why Refrigerant 22 Should be Favored for Absorption Refrigeration," ASHRAE J., December 1959, pp.45-50.

13. Carlson, H.C., and A.P. Colburn, "Vapor-Liquid Equilibria of Nonideal Solutions," Ind. Eng. Chem., Vol.34, No.5, May 1942, pp.581-589.

14. Hala, E., J. Pick, V. Fired, and O. Vilim, Vapour-Liquid Equilibrium, Second English Ed., Pergamon Press, 1967.

15. Colburn, A. P., and E. M. Schoenborn, "The Selection of Separating Agents for Azeotropic and Extractive Distillation and for Liquid-Liquid Extraction," Transactions of the A.I.Ch.E., Vol. 16, 1945, pp. 421-443.

16. Mastrangelo, S. V. R., "Solubility of Some Chlorofluorohydrocarbons in Tetraethylene Glyco Dimethyl Ether," ASHRAE J., October 1959, pp. 64-68.

17. Blutt, J. R., and S. E. Sadek, "A Gravity Independent Vapor Absorption Refrigerator," NASA CR-836, Dynatech Corp., July 1967.

18. Mastrangelo, S. V. R., "Equation of Solubility of Nonelectrolytes which Possess a Specific Interaction," J. Phys. Chem., 63, pp. 608-63, 1959.

19. Zellhoefer, G. F., and M. J. Copley, "The Heats of Mixing of Haloforms and Polyetheylene Glycol Ethers," J. Am. Chem. Soc., 60-1, pp. 1343-1345, June 1938.

20. Shaffer, A., "Analytical Methods for Space Vehicle Atmospheric Control Processes," Airesearch Mfg. Co., Los Angeles, Calif., ASD 61-162, Part I, December 1961.

21. Feldmanis, C. H., "Performance of Boiling and Condensing Equipment under Simulated Outer Space Conditions," ASD-7DR-63-862, Wright-Patterson Air Force Base, Ohio, November 1963.

22. Costello, C., and E. Redeker, "Boiling Heat Transfer and Maximum Heat Flux for a Surface with Coolant Supplied by Capillary Wicking," Chemical Engineering Progress Series, Heat Transfer, Vol. 59, No. 41, 1963.

23. Ginwala, K., T. A. Blatt and R. W. Bilger, "Engineering Study of Vapor Cycle Cooling Components for Space Vehicles." ASD-TDR-63-582, Wright-Patterson Air Force Base, Ohio, September 1963.

24. "Evaluation and Performance of Once-Through Zero-Gravity Boiler Tuves with Two-Phase Water," Pratt & Whitney Report AC-428, July 1964.

25. Ginwala, K., et al., "Engineering Study of Vapor Cycle Cooling Equipment for Zero-Gravity Environment," WADD TR 60-776, Northern Research Engineering Corp., January 1961.

26. Engle, W., and G. Scott (Editors) "Development, Fabrication and Testing of Honeycomb Radiator Condenser," Atomic International, NAA-SR-9885, December 1964.

27. "Multi-Tube Boiler and Condenser Capsule Design Study Report," TRW Equipment Laboratory, Air Force Technical Report AFAPL-TR-66-150, March 1967.

28. "Development of a Refrigeration System for Lunar Surface and Spacecraft Applications," LMSC-D080861, Lockheed Missiles & Space Company, Lockheed Palo Alto Research Laboratory, Calif., May 1969.

29. Kays, W.M., and A.L. London, Compact Heat Exchangers, second edition, McGraw-Hill Book Company, New York, 1964.

30. Eckert, E.R.G., and R.M. Drake, Jr., Heat and Mass Transfer, second edition, McGraw-Hill Book Company, New York, 1959, p. 211.

31. McAdams, W.H., Heat Transmission, third edition, McGraw-Hill Book Company, New York, 1954, pp. 242-243.

32. Kreith, F., and D. Margolis, "Heat Transfer and Friction in Turbulent Vortex Flow," Appl. Sci. Res., Section A, 8, 1959, p. 457.

33. Uchida, H., and S. Yamaguchi, "Heat Transfer in Two-Phase Flow of Refrigerant 12 through Horizontal Tube," Proc. Third Inter. Heat Transfer Conf., Fol. 5, 1966, pp. 69-79.

34. Sadek, S.E., and L.G. Clawson, "Evaluation of a Gravity-Independent Vapor Refrigerator," Final Report on Contract NAS9-7948, Dynatech R/D Company, 31 October 1968.

35. Liu, C.K., Lockheed Missiles & Space Company IDC TP-3158, 28 December 1970.

Section 11
TABLES AND FIGURES

Table 1

SURVEY OF INORGANIC AND HALOGENATED ORGANIC REFRIGERANTS

Fluid	Chemical Formula	Refrigeration Code R	Flammable	Explosive	UWL* Class < 5	ASA** Hazard > 1
Carbon Dioxide	CO_2	744				
Ammonia	NH_3	717	x	x	x	x
Nitrous Oxide	N_2O	744a				
Sulfur Hexafluoride	SF_6	7146				
Sulfur Dioxide	SO_2	764			x	x
Water	H_2O	718				
	$CF Cl_3$	11				
	CF_2Cl_2	12				
	CF_3Cl	13				
	CF_3Br	13B1				
	CF_4	14				
	$CHFCl_2$	21	x		x	
	CHF_2Cl	22				
	CHF_3	23				
	CH_2Cl_2	30	x	x	x	
	CH_3Cl	40	x	x	x	x
	$CFCl_2 \cdot CF_2Cl$	113			x	
	$CF_2Cl \cdot CF_2Cl$	114				
	$CF_3 \cdot CF_2Cl$	115				
	$CH_3 \cdot CF_2Cl$	142	x		x	
	$CH_3C Cl F_2$	142b	x			
	$CH_3 \cdot CHF_2$	152	x			
	$CH_3 CHF_2$	152a	x			
	$C_3F_6 Cl_2$	216				
	C_4F_8	C318				
	CH_3CH_2Cl	160		x		x
	$HCOOCH_3$	611		x		x
	$CH Cl = CH Cl$	1130		x		x
	$CH_3 \cdot CF_3$	143	x			

NOTES:

Data taken from Refs. 1 and 2

*UWL   Underwriters' Lab group classification (1-6): 1 = most toxic, 6 = least toxic

**ASA   Aerosol classification (1-3):   1 = least hazardous, 3 = most hazardous.

11-1

Table 2

TEST DESIGN CONDITIONS

Location	Temperature ($^{\circ}F$)	Pressure (psia)	Absorbent Enthalpy (Btu/lb_m)	Refrigerant Enthalpy (Btu/lb_m)	Absorbent Flow Rate (lb_m/min)	Refrig. Flow Rate (lb_m/min)	Mole Fraction Refrig.
1*	40.0	83.9	—	109(v)	0	27	1.00
2	109.2	83.9	—	121(v)	0	27	1.00
3	138.5	83.9	80	55(ℓ)	340	163	0.55
4	242.0	247.7	126	86(ℓ)	340	163	0.55
5	250.0	247.7	130	89(ℓ), 140(v)	340	163	0.55
6	110.5	247.7	—	46(ℓ)	0	27	1.00
7	141.9	247.7	81	56(ℓ)	340	136	0.51
8	82.0	247.7	—	34(ℓ)	0	27	1.00
9	138.5	247.7	80	55(ℓ)	340	163	0.55
10	250.0	247.7	—	140(v)	0	27	1.00
11	250.0	247.7	130	89(ℓ)	340	136	0.51
12	40.0	83.9	—	34(ℓ+v)	0	27	1.00
13	141.9	83.9	81	56(ℓ)	340	136	0.51

q_g = 57 kW = 3253 Btu/min

q_{abs} = 53 kW = 2996 Btu/min

q_{rec} = 368 kW = 20908 Btu/min

q_{sub} = 6 kW = 325 Btu/min

q_{cond} = 44 kW = 2506 Btu/min

q_{pump} = 4 kW = 232 Btu/min

w_{ev} = 55 lb w_{cond} = 1326 lb

w_{abs} = 1215 w_{sub} = 16 lb

w_{pump} = 159

w_{rec} = 359

w_g = 286

*Numbers correspond to points on Fig. 20

NOTES: Fluids = R-22/DME-TEG

$q_{incident}$ = 50 Btu/hr-ft^2

q_{evap} = 35 kW = 1991 Btu/min

Absorber and Generator Efficiency = 80%

Absorber Radiator Area = 608 ft^2 on each side

Condenser = 663 ft^2 on each side

v = vapor

ℓ = liquid

WD = 2.0 lb/ft^2

Table 3

ABSORBER TEST RESULTS

	Test Run 12-31-70		Test Run 01-04-71	
Weak Solution Tank				
Liquid temp., $^\circ$F	145		147	
Supply pressure, psi	110		110	
Liquid capacity, lb.				
Before Test	117.2		82.9	
After Test	86.2		66	
Absorber Inlet – Weak Solution				
Temperature, $^\circ$F	142		143	
Pressure, psi	110		110	
Flow rate, lb/min	8.97	$\pm$ .42	8.97	$\pm$ .42
Absorber Inlet – R-22 Vapor				
Temperature, $^\circ$F	110		110	
Pressure, psi	69.2	+0.2	69.2	$\pm$ 0.2
Flow rate, lb/min	.5	$\pm$ .02	.5	$\pm$ .02
Weak Solution Sample				
Temperature, $^\circ$F	85		85	
Refrigerant concentration	.508		.508	
Absorber Exit – Strong Solution				
Temperature, $^\circ$F	124°F		124°F	
Pressure, psi	68.2	$\pm$ 2.0	68.2	$\pm$ 2.0
Strong Solution Sample				
Temperature, $^\circ$F	85		89	
Refrigerant Concentration	0.61		0.56	
Absorber Cooling Water				
Inlet temperature, $^\circ$F	123		123	
Outlet temperature, $^\circ$F	126		126	
Flow rate, lb/min	11		11	

Table 4

SCENARIO FOR COMPANION MOTION PICTURE

Film Title:	Evaluation of Absorption Cycle for Space Station Environmental Control System Application
Type of Film:	16 mm, black and white, silent. Speed: 24 frames/sec

Scene	Subject
Part I	Absorber Test Apparatus
I-1	E-181 Container, E-181 Pressure Tank - Filling Valve, Relieve Valve, GHe Line, Pressure Gage, Bleed Valve, Dial Thermometer and Discharge Valve.
I-2	Weak Solution Mixing Tank - E-181 Inlet Valve, R-22 Inlet Valve, Weak Solution Discharge Valve
I-3	R-22 Inlet to Mixing Tank, Charging Cylinder Valve, Inlet Valve from Liquid R-22 Line
I-4	Weak Solution Mixing Tank - Liquid R-22 Inlet Valve, Weak Solution Supply Line to Absorber, E-181 Inlet Valve
I-5	Weak Solution Mixing Tank - Dial Thermometers, View Glass Indication Tank Capacity, Air Motor Coupled to Stirrer Bleed Valve, GHe Line
I-6	Tank Pressure Gage
I-7	Weak Solution Mixing Tank - GHe Valve, Vacuum Valve, Bleed Valve, Relief Valve and Drain Line.

11-4

Table 4 (Continued)

Scene	Subject
I-8	Weak Solution Drain Line, Weak Solution Supply Line to Absorber.
I-9	R-22 Vapor Supply - R-22 Containers with Heating Tapes, Relief Valve and Pressure Regulators, Immersion Heating Baths, R-22 Rotameter
I-10	Weak Solution Supply - Weak Solution Rotameter Weak Solution Sampling Station - Bleed and GHe Valves
I-11	Absorber from Inlet to Exit, Insulated Absorber Line, Bare Return Line to Dump Tank.
I-12	Absorber Exit - View Section with Safety Shield, Return Line, Sampling Station, Coolant Inlet Valve, Rotatmeter and Dial Thermometer
PART II	Flow Pattern at Absorber Exit
	Begin with clear weak solution flow followed by two-phase flow as R-22 vapor was introduced and both flow rates were adjusted.
	End with clear strong solution flow.

Table 5

ABSORBER AND GENERATOR TEST RESULTS

Absorber Inlet

      R-22 Vapor: Flow rate,   0.187 lb/min
                                 Temperature,   100 $^\circ$F
                                 Pressure,   75 psia

      Weak Solution: Flow rate,   5.05 lb/min
                                 Temperature,   110 $^\circ$F
                                 Pressure,   125 psia
                                 Mol-concentra-   0.52
                                   tion

Absorber Exit

      Strong Solution: Temperature,   90°F
                                 Pressure,   70 psia
                                   Mol-concentra-   0.55
                                   tion

Absorber Coolant:

                                 Inlet temperature, 80°F
                                 Inlet flow rate,   8.75 lb/min
                                 Exit temperature,   100°F

Recuperator

      Strong Solution: Inlet Temperature, 120°F
                                 Exit Temperature,   180°F

      Weak Solution: Inlet Temperature, 200°F
                                   Exit Temperature,   150°F

Generator

                                 Inlet Pressure,   185 psia
                                 Inlet Temperature, 180 $^\circ$F
                                 Exit Temperature   220°F
                                 Power Input   2.18 KW

Table 6

DETERMINATION OF SPECIFIC GRAVITY OF ANSUL E-181 AT
VARIOUS TEMPERATURES, GRAVIMETRIC RESULTS

Calibration of Pycnometer Bottles (76°F)

	Bottle No. 1	Bottle No. 2
Tare, GM	20.4320	19.0478
$\bar{C}$ H_2O GM	45.3505	43.9595
Net H_2O GM	29.9185	24.9117

Specific Gravity E-181 (ANSUL), (H_2O @ 76°F)

Temp.			Bottle No. 1	Bottle No. 2
76°F	Gross		45.5775	44.2032
	Tare	Net	20.4320	19.0478
			25.1455	25.1559
	Sp.G.		1.009	1.009
268°F	Gross		43.2041	41.8305
	Tare	Net	20.4320	19.0478
			22.7721	22.7827
	Sp.G.		0.914	0.914
179°F	Gross		44.3995	42.9690
	Tare		20.4320	19.0478
		Net	23.9675	23.9212
	Sp.G.		0.962	0.961
227°F	Gross		43.7223	42.3520
	Tare	Net	20.4320	19.0478
			23.2903	23.3042
	Sp.G.		0.935	0.935
117°F	Gross		45.0746	43.7043
	Tare		20.4320	19.0478
		Net	24.6426	24.6565
	Sp.G.		0.989	0.990

Table 7

GRAVITY INDEPENDENT ABSORBERS

Design Concepts	A Ejector Absorber	B Vortex Type	C Vortex-Ejector
Reference	(17)	(21), (28)	(21), (28)
Mass Transfer	Refrigerant vapor enters directly into the tube while the absorbent liquid is sprayed into the vapor through a small concentric nozzle at high relative velocity.	High pressure absorbent is sprayed radially through fine holes in the inner tube of a concentric tube into the refrigerant vapor flowing axially through the annular space.	The absorbent is injected axially through the outer tube wall of a concentric tube into the refrigerant vapor flowing in the annular space.
Heat Transfer	The flow tube is integral with radiator fin.	The outer tube is integral with radiator fin.	Coolant flows in inner tube.
Discussion	Mixing is enhanced by high relative velocity which also serves to pump the mixture down the flow tube.	There is no pumping action of axial absorbent injection but mixing is further enhanced by increased turbulence. Twisted tapes or wires are needed in annular space.	Pumping action of absorbent is used along with twisted tapes or wires.

Recommended concept - Concept B represents the best design in the mass transfer process which makes heat transfer as the limiting factor. The operation will be similar to a condenser where data are available. It also has higher condensation film coefficient as vapor is condensed inside tubes (Ref. 21). In the present experiment, an assembly of small diameter tubes can be attached thermally to one side of a high conductivity flat plate whose other side is cooled by coolant circulating through attached coils.

Unlisted Design Concepts

Reference

a. Tapered inner tube concept (21)
b. Rotating-centrifugal Disc Concept (25)
c. Spiral Type (25)
d. Steel Honeycomb Type (26)

Table 8

GRAVITY INDEPENDENT GENERATORS

Design Concept.	A Wick Lined Tube with Separator	B Vortex Generator	C Serpentine Tubes
Reference	(17) (22) (23)	(17),(21),(23),(24),(25)	(24)
Description	A porous wicking material lining the tube wall keeps the liquid in contact with the tube wall by surface tension.	Flow motion is caused by inertial force generated by twisted ribbons or helical inserts.	A bundle of serpentine tubes is put in packaging form to incorporate the features of simple tube support and straight shell construction.
Heat Transfer	It has higher burn-out heat flux but has lower overall heat transfer rate for a given temperature difference.	Interchange of the phases is enhanced at the inner tube wall and resulted in higher heat transfer coefficient.	Good heat transfer characteristics obtained in tests.
Discussion	This system requires higher temperature source but the liquid is always held in control and no independent separator is needed.	This system needs an independent separator. Higher pressure drop required shorter length of tube.	This system needs an independent separator. It has low pressure drops but complexities in fabrication.

Recommended concept - Concept B using twisted ribbons is recommended for its simplicity and relative ease of fabrication. Small tubes in parallel can be attached thermally to a flat plate of high thermal conductivity whose reverse side is heated by electrical heating elements. Heat transfer coefficients and pressure drop data are available.

Unlisted Design Concepts	Reference
a. Internally-finned tubes	(24)
b. Dual-diameter Tubes	(24)

11-9

Table 9

METHODS OF HEAT ADDITION TO THE GENERATOR (DESORBER)

	Methods	Description
(A)	Solid Conduction	The generator tubes are imbedded in a large block of metal heated by isotope or electrical elements which are loaded in bored holes in the block. The heat block also provides a large portion of the shielding for an isotope heat source.
(B)	Liquid Conduction	The tube coil and heating elements are both contained in a molten bath of high conductivity fluid like NaK. There may be difficulties in fuel handling.
(C)	Two-loop boiler	An auxiliary loop is used to circulate a coolant between the heat source and a two-fluid shell and tube boiler and the heat is then transferred to the cycle fluid in the generator. This concept involves added components, weight and complexity.
(D)	Radiation	Heat is transferred by radiation from the heat source to the generator coil which is physically separated from the former.

Table 10

GRAVITY INDEPENDENT SEPARATORS

Design Concept	A Surface Tension Type	B Centrifugal Type	C 2-stage Type
Reference	(17)	(17), (25)	(28)
Description	The inlet flow passes through a wicking "sock" where liquid droplets are caught by the wick and the vapor allowed to pass through the liquid is then sucked out of the wick.	A centrifugal force field is used to separate the denser liquid from the vapor. The former is trapped by a sponge, wick or mesh material to be removed by capillary action, pressure differential or mechanical expression of the wick material.	Inertial effects as produced by flow swirling are used in the upstream portion to remove the larger particles while wick techniques are used in the downstream section to remove the entrained liquid.

Recommendations: In the present investigation, concept A is recommended for its stable operation and good correlation to analytical predictions.

Unlisted Design Concepts

		Reference
a.	Electrohydrodynamics Separator	(17)
b.	Electrostatic Separator	(25)
c.	Acoustic Device	(25)
d.	Impingement Separator	(25)
e.	Straight-through flow with conical screen whose apexes point upstream	(28)
f.	Flow Reversal Type	(28)
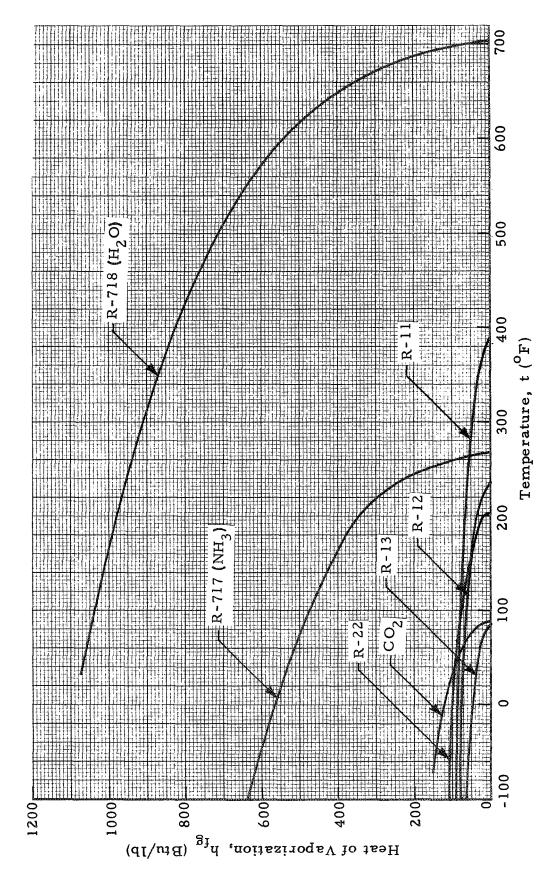
Fig. 1 - Heat of Vaporization of Typical Organic and Inorganic Refrigerants
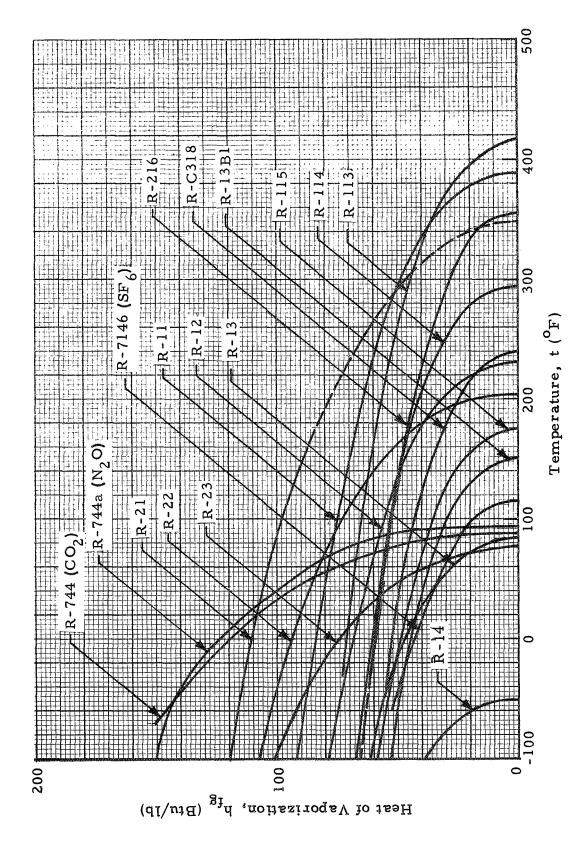
11-12

Fig. 2 - Heat of Vaporization of Various Refrigerants

R	$\left(\dfrac{p - p^o}{p^o}\right)_{max}$
11	+ 0.143
12	+ 0.364
21	- 0.6
22	- 0.575
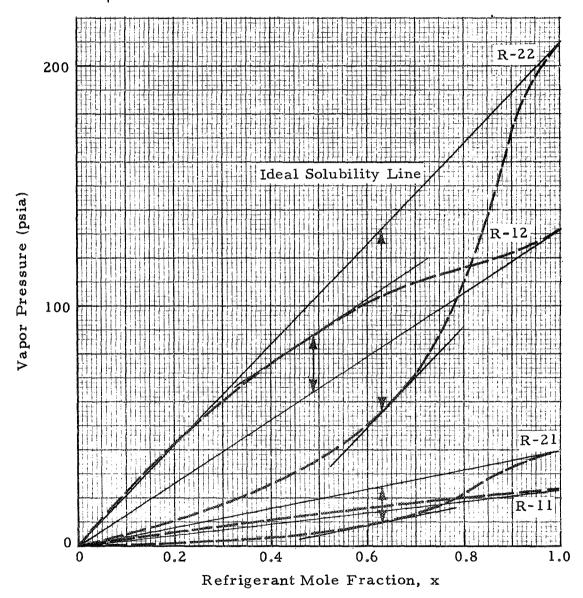
Fig. 3 - Solubility of Refrigerants 11, 12, 21 and 22 in DME-TEG (t = 100°F)
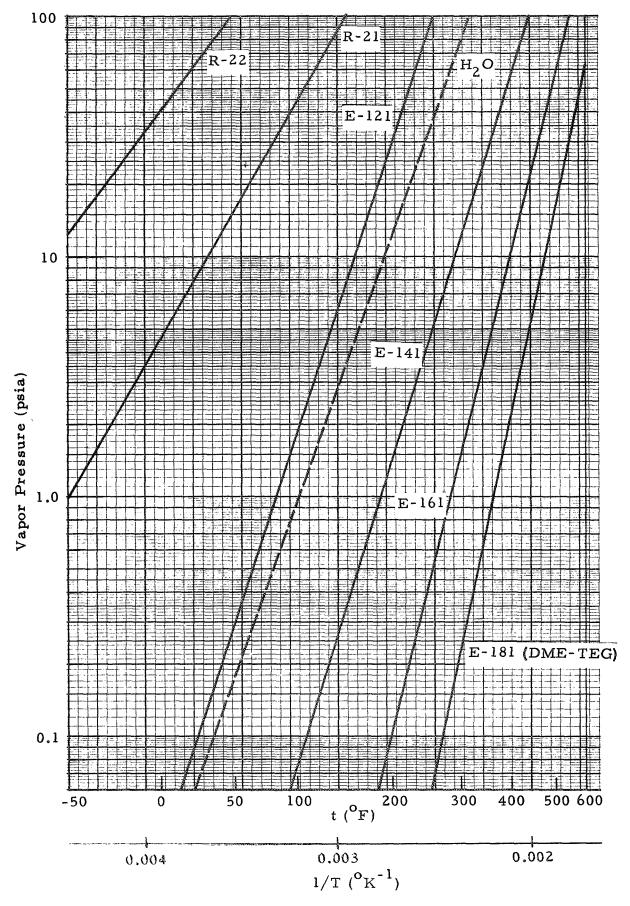
Fig. 4 - Vapor Pressures of Typical Absorbents and Refrigerants
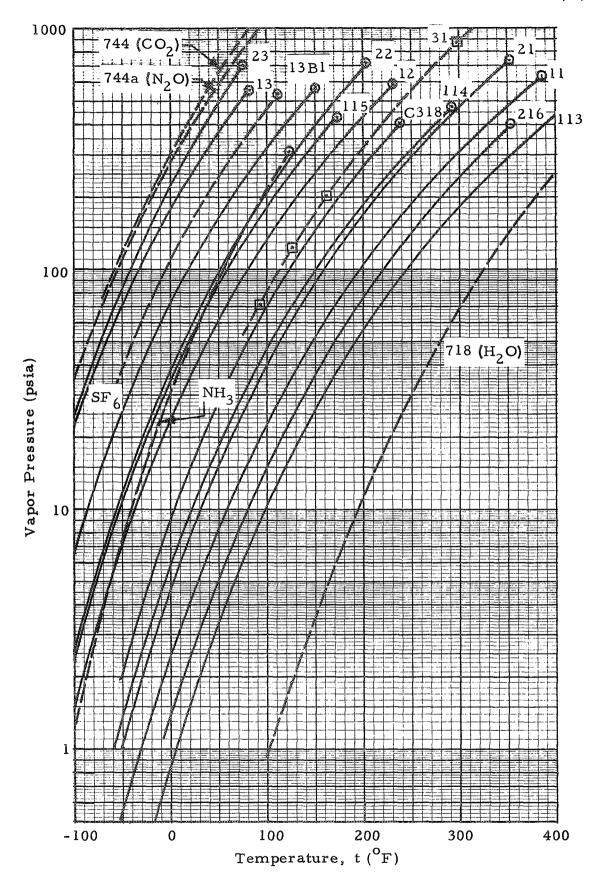
Fig. 5 - Vapor Pressures of Various Refrigerants

11-16
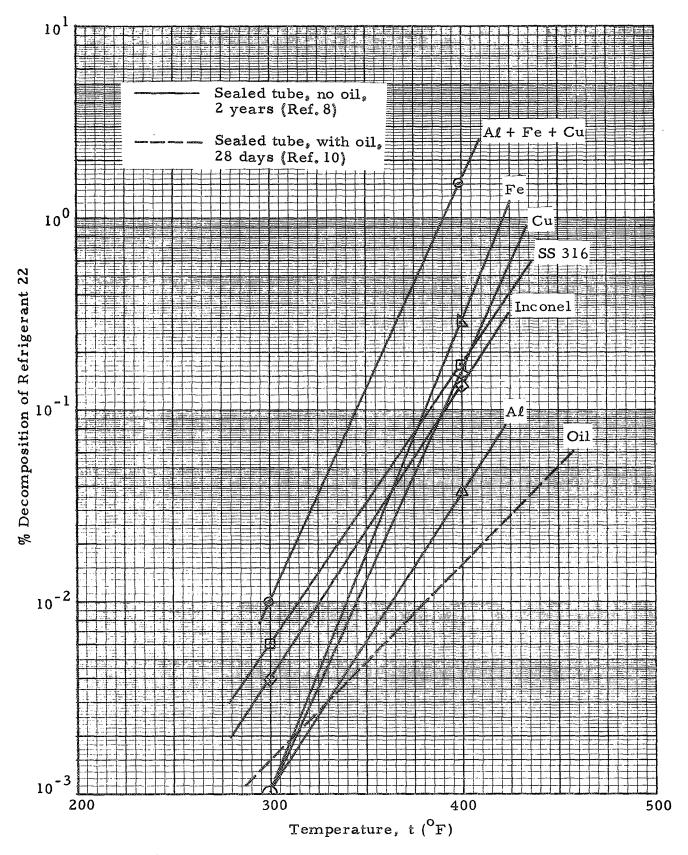
Fig. 6 - Effect of Temperature and Contaminants on Total R-22 Decomposition

11-17
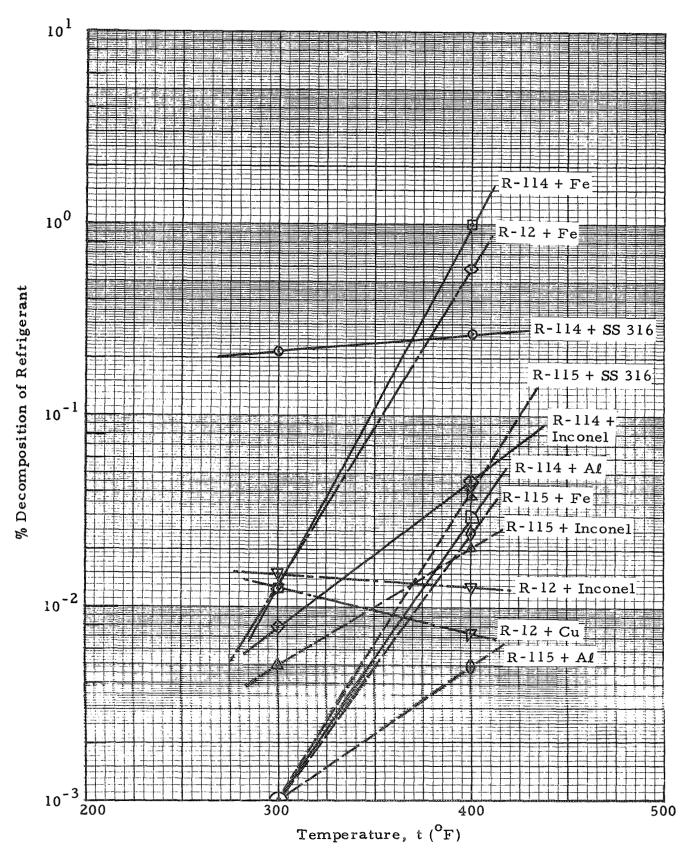
Fig. 7 - Stability of R-12, R-114 and R-115 with Metals (Ref. 8;
Sealed Tube, No Oil, 2 Years)

11-18
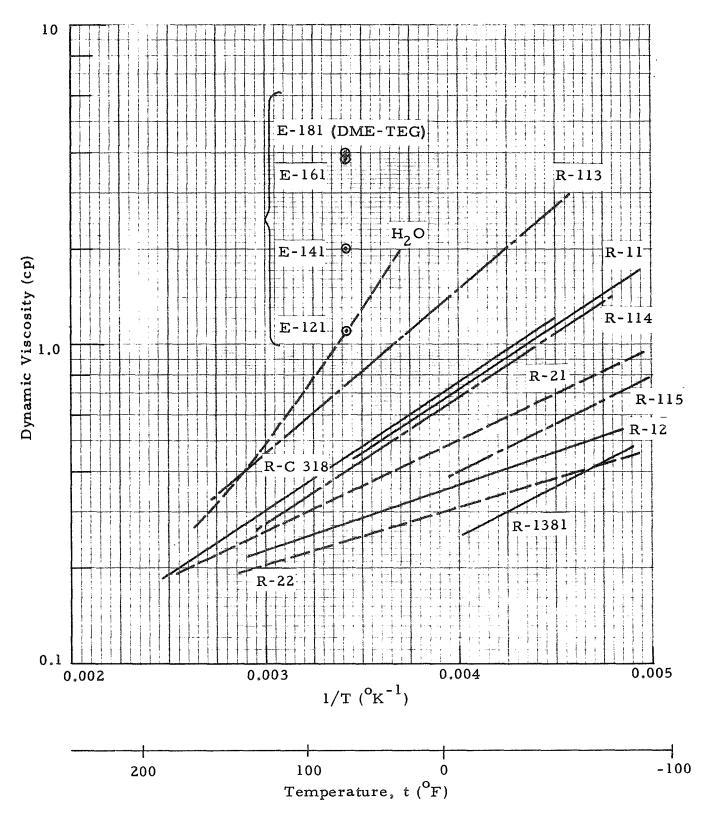
Fig. 8 - Liquid Viscosities of Various Absorbents (Ref. 7)
and Refrigerants (Ref. 11)
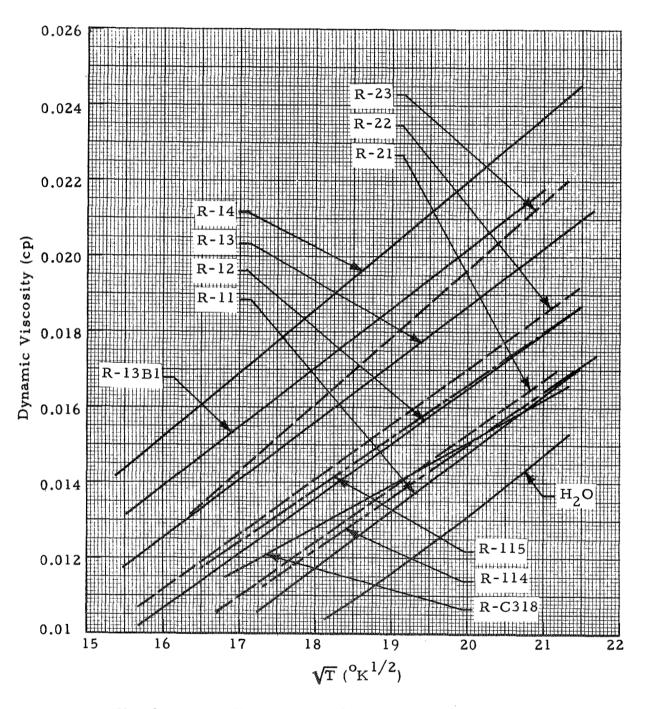
Fig. 9 - Vapor Viscosities of Various Refrigerants (Ref. 11)
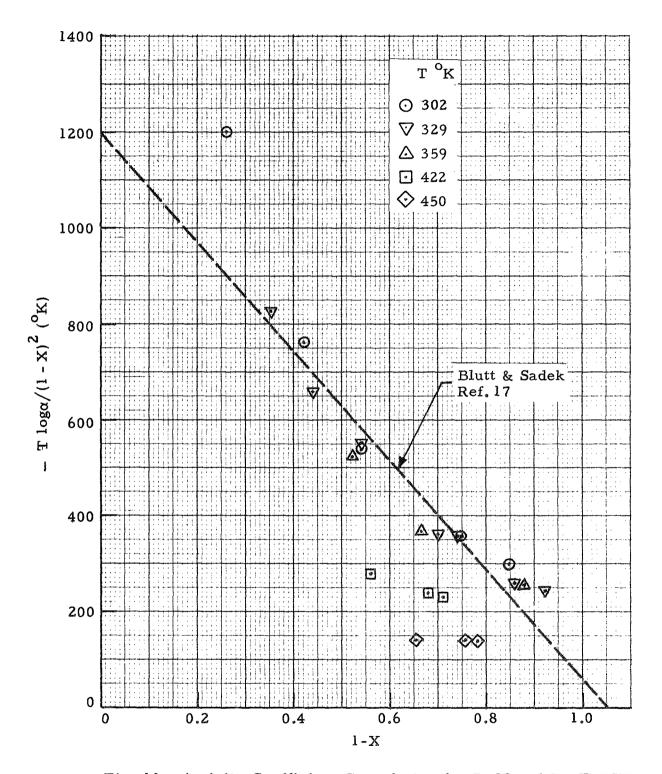
Fig. 10 - Activity Coefficient Correlation for R-22 and DME-TEG
(Data from Ref. 16)
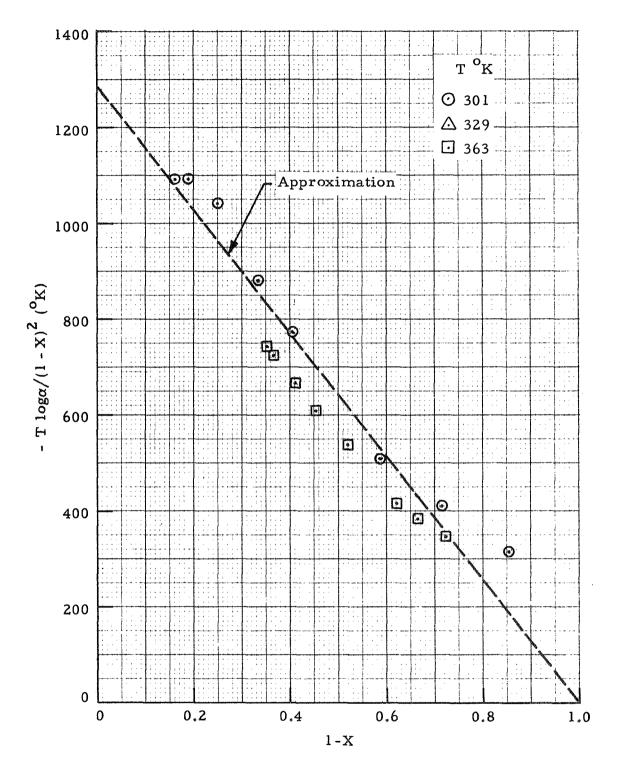
Fig. 11 - Activity Coefficient Correlation for R-21 and DME-TEG
(Data from Ref. 16)
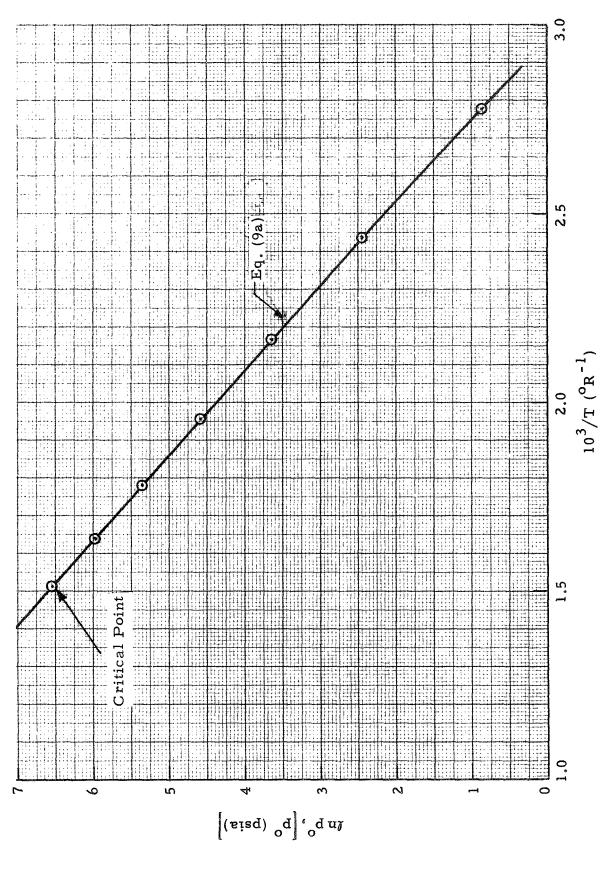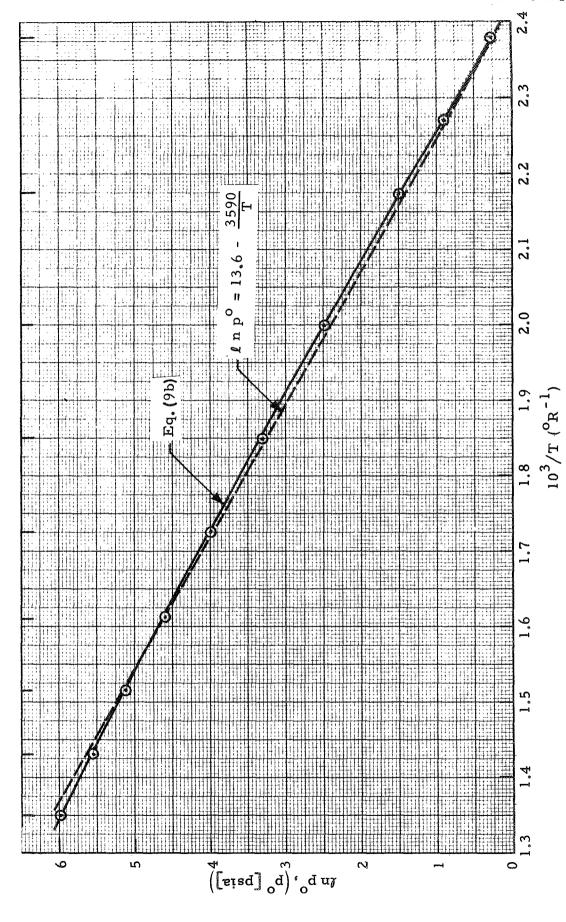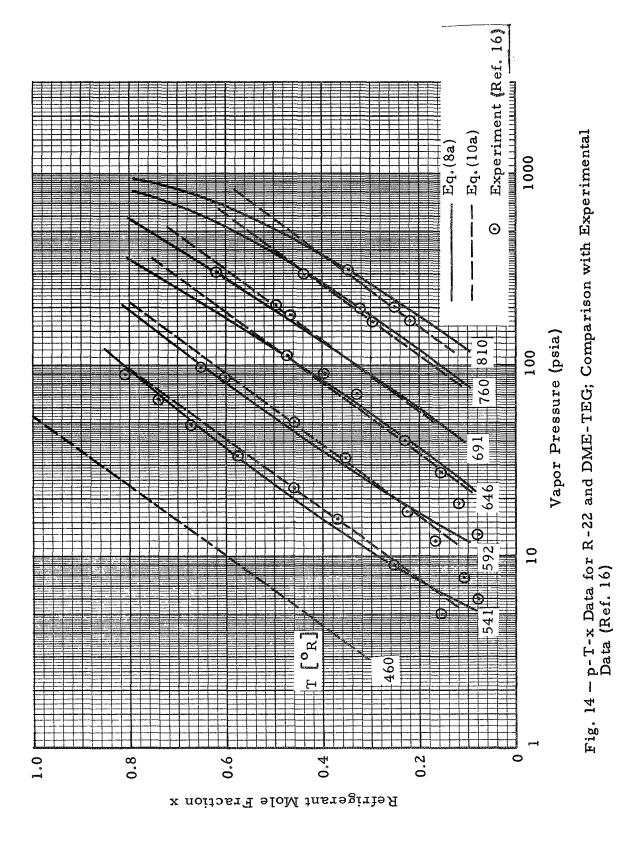
Fig. 12 - Vapor Pressure of Refrigerant 22

Fig. 13 - Vapor Pressure of Refrigerant 21

LOCKHEED-HUNTSVILLE RESEARCH & ENGINEERING CENTER

Fig. 14 — p-T-x Data for R-22 and DME-TEG; Comparison with Experimental
Data (Ref. 16)
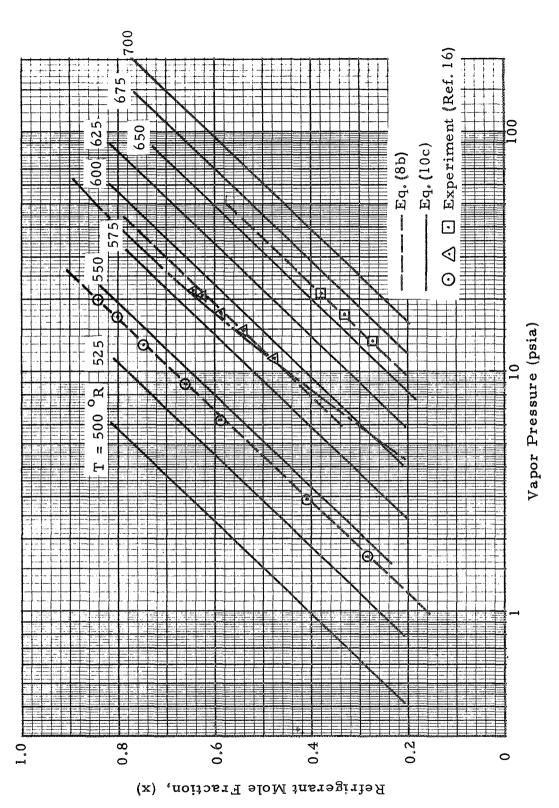
Fig. 15 - p-T-x Data for R-21 and DME-TEG; Comparison with Experimental Data (Ref. 16)

———————— Eq. (11a)

———————— Ref. 3

— ———— — ———— Constant spec. heat
$C_p = 0.306$ (Btu/lb^{o}R)
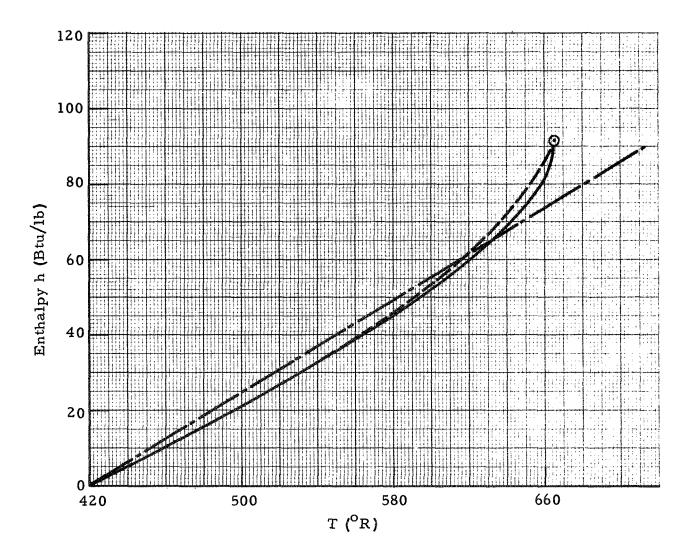
Fig. 16 — Enthalpy of Saturated Liquid Refrigerant 22
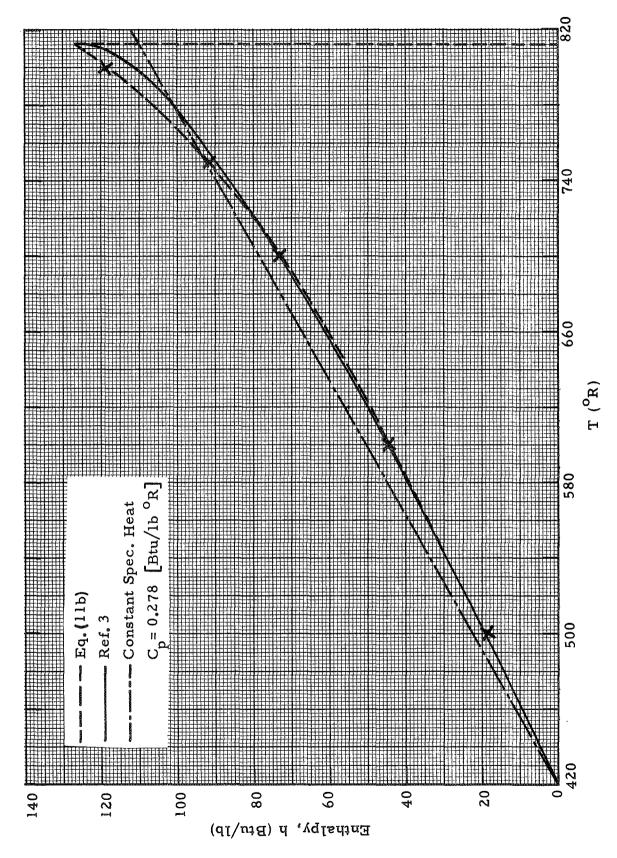
Fig. 17 - Enthalpy of Saturated Liquid Refrigerant 21

LOCKHEED - HUNTSVILLE RESEARCH & ENGINEERING CENTER
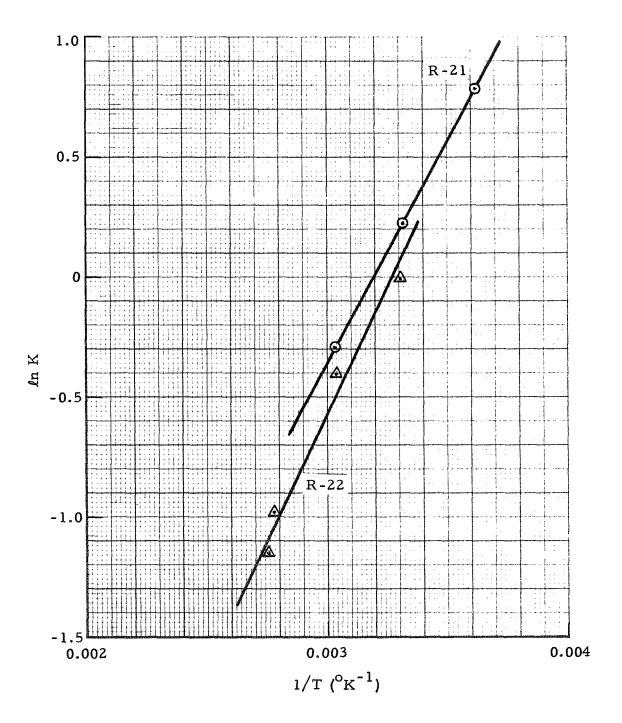
Fig. 18 — Equilibrium Constant K as Function of Temperature for R-21 and R-22
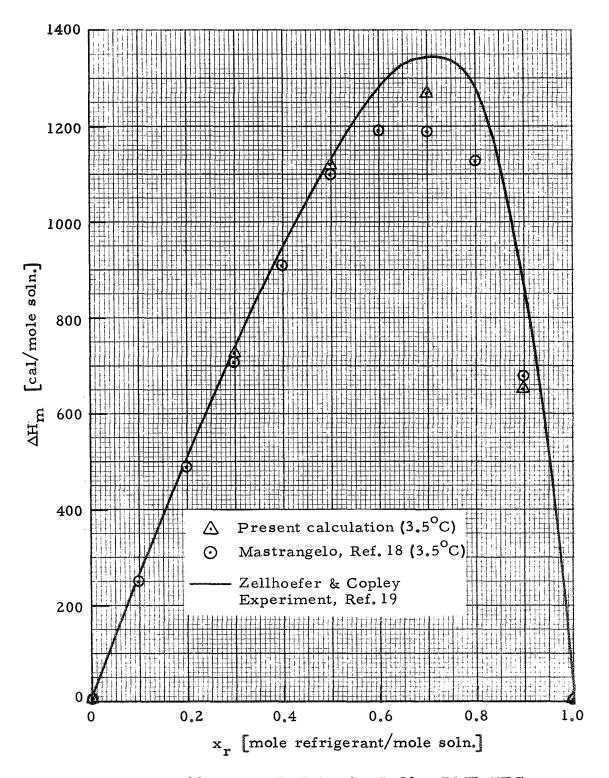
Fig. 19 - Heat of Mixing for R-21 & DME-TEG

NOTE: Throttle valves are isenthalpic, separator is isenthalpic and isothermal, pump is isenthalpic and isothermal.
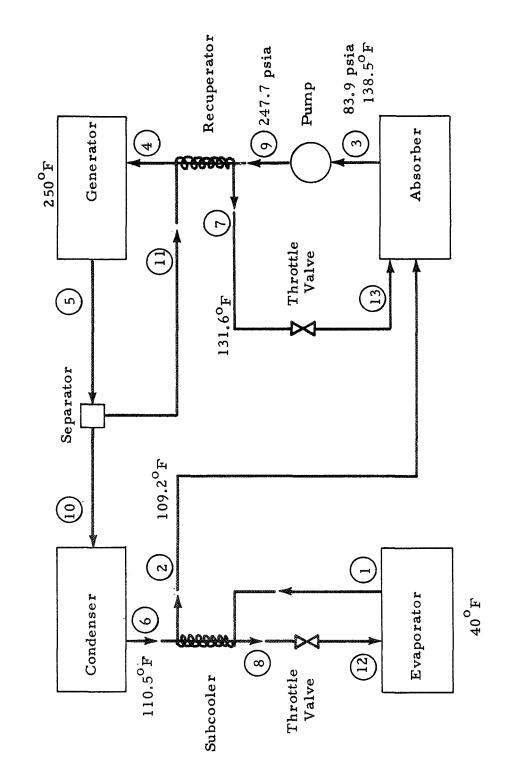
Fig. 20 – Absorption Refrigeration Cycle Schematic
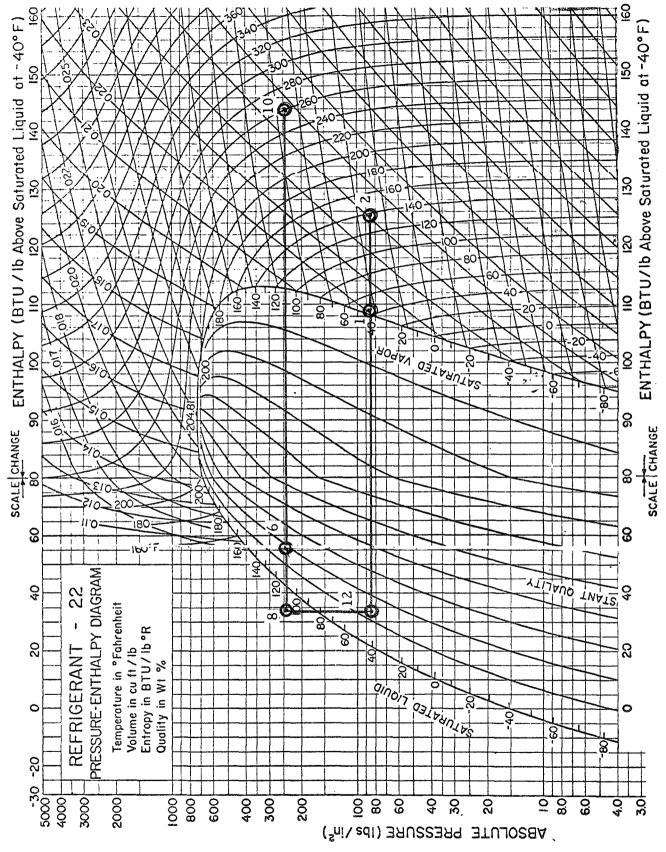
Fig. 21 — Pressure Enthalpy Diagram for Refrigerant 22
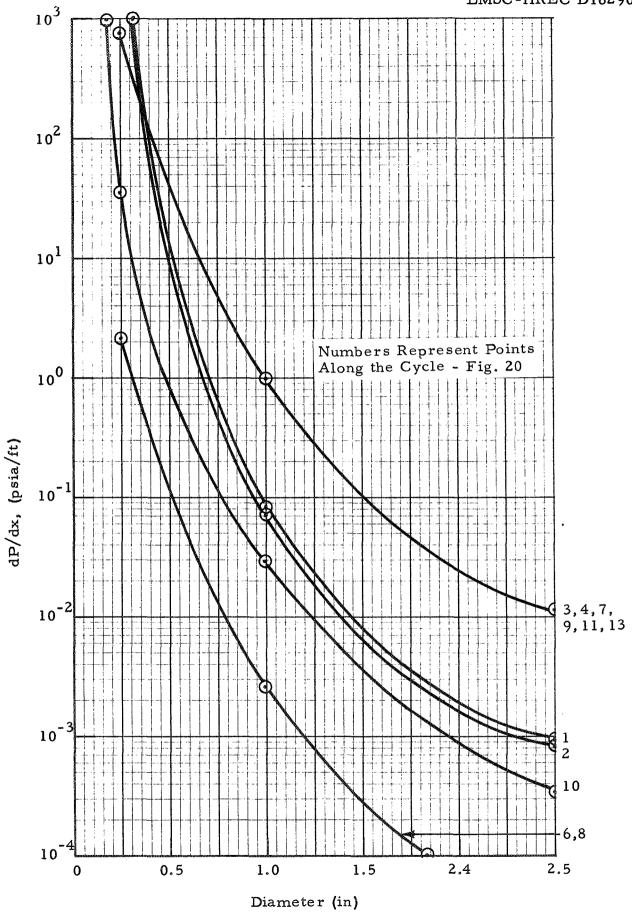
Fig. 22 — Pressure Gradients Along Refrigeration Cycle
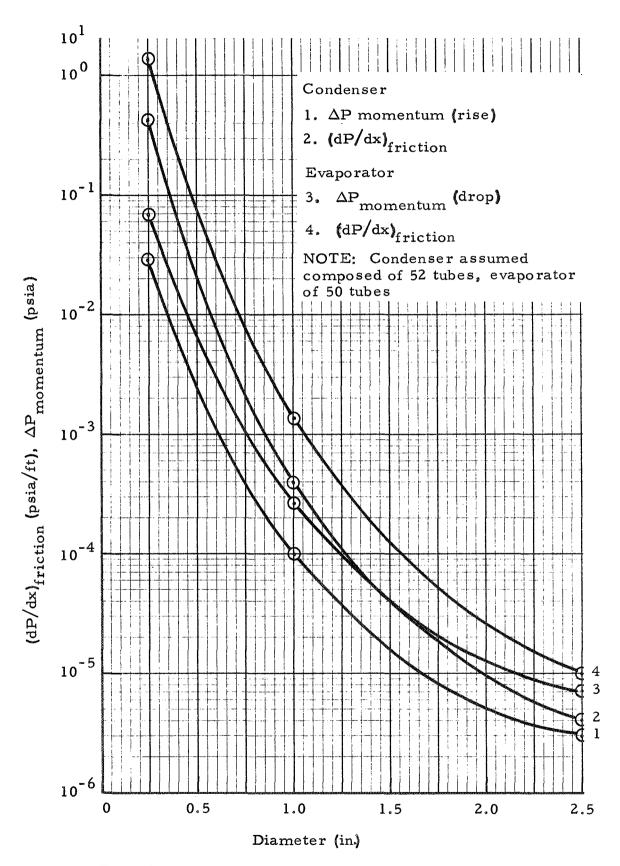
Fig. 23 — Condenser and Evaporator Pressure Gradients
and Pressure Changes Due to Momentum Changes

11-34
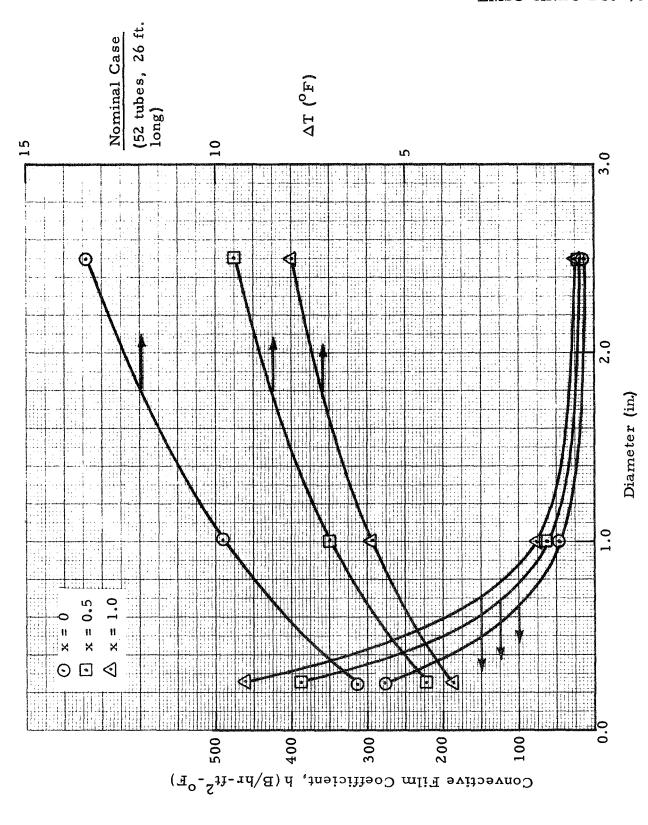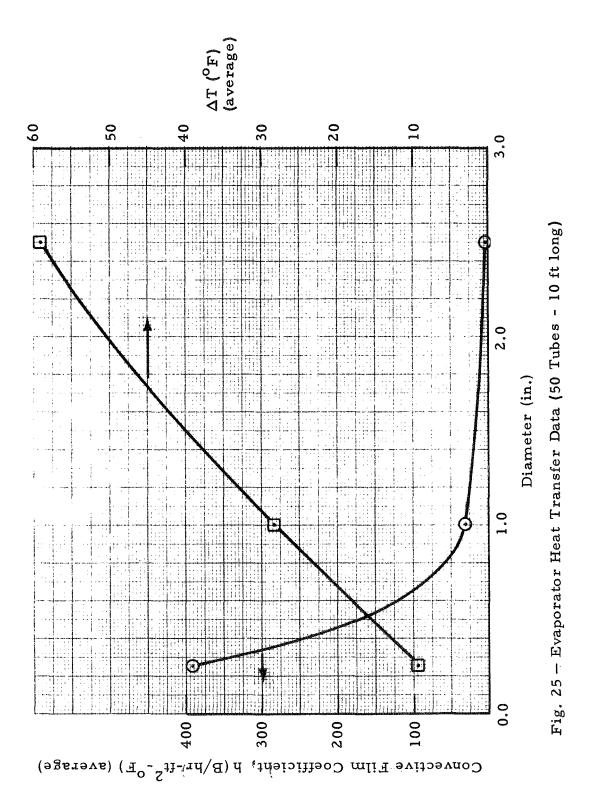
Fig. 24 – Condenser Heat Transfer Data

Fig. 25 — Evaporator Heat Transfer Data (50 Tubes – 10 ft long)
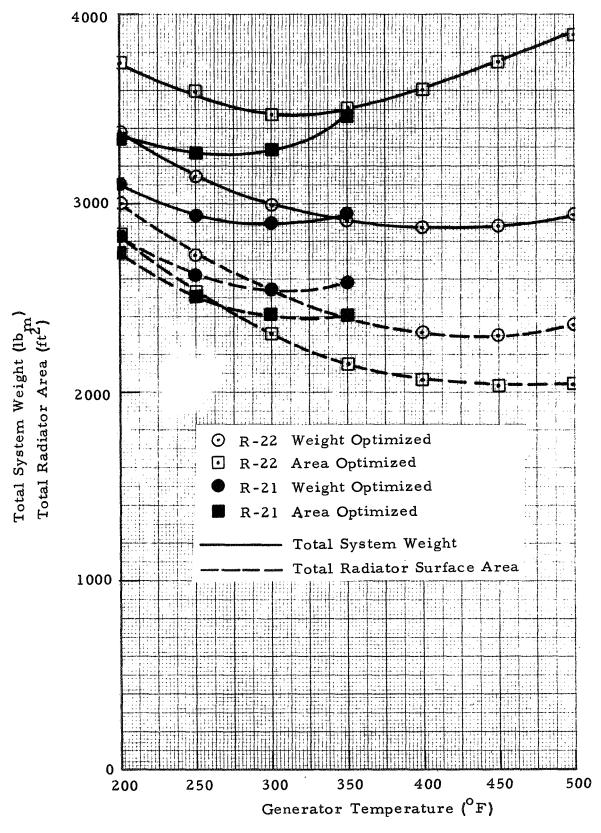
Fig. 26 — Optimized System Weight and Radiator Area
Dependence on Generator Temperature

11-37
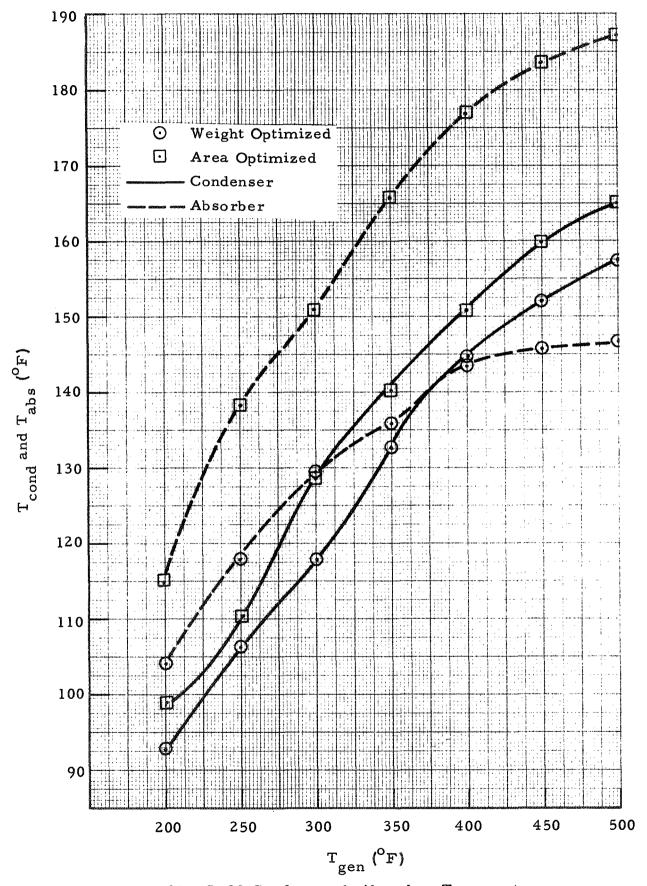
Fig. 27 — R-22 Condenser & Absorber Temperatures

11-38
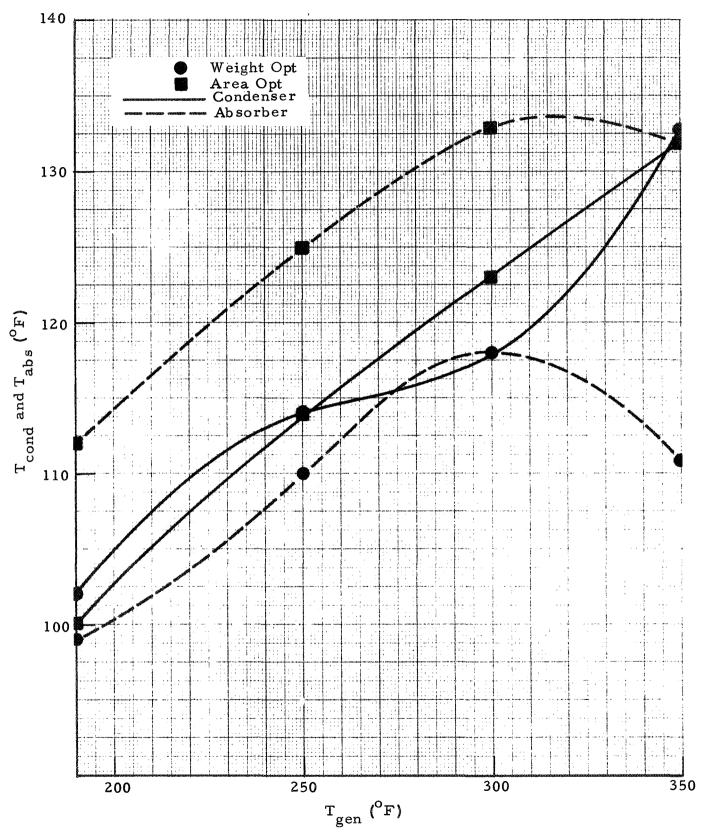
Fig. 28 — R-21 Condenser and Absorber Temperatures
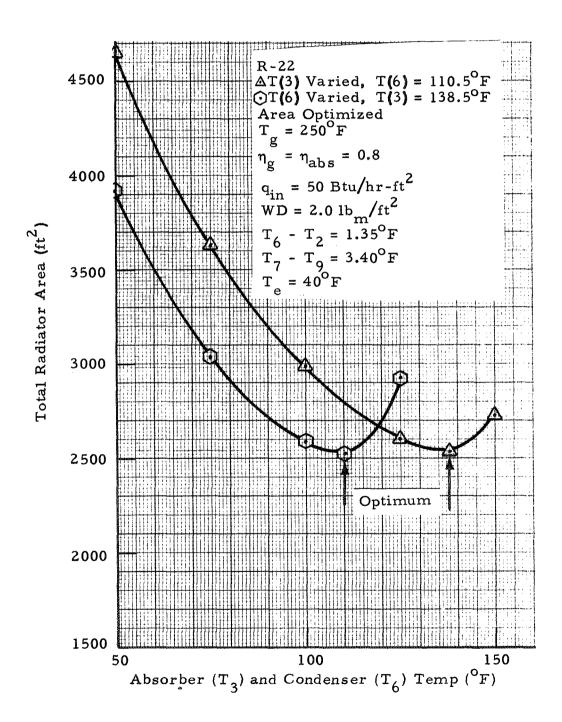
Fig. 29 — Effect of Varying Absorber and Condenser
Temperatures From Their Optimum Values

11-40

R -22
Area Optimized
$T_g = 250^{\circ}F$

$T_e = 40^{\circ}F$

$\eta_{abs} = \eta_g = 0.8$

$q_{in} = 50 \text{ Btu/hr-ft}^2$

$T_6 - T_2 = 1.35^{\circ}F$

$T_7 - T_9 = 3.40^{\circ}F$
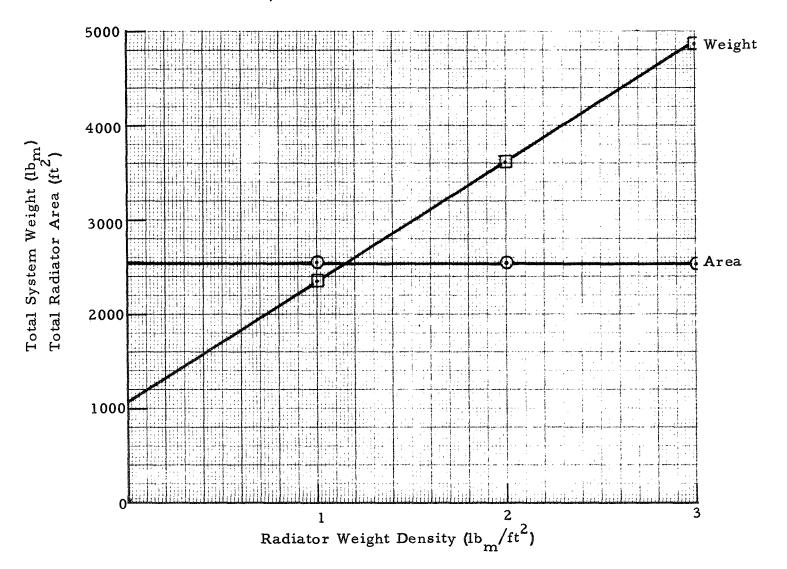
Fig. 30 — Effect of Varying Radiator Weight Density
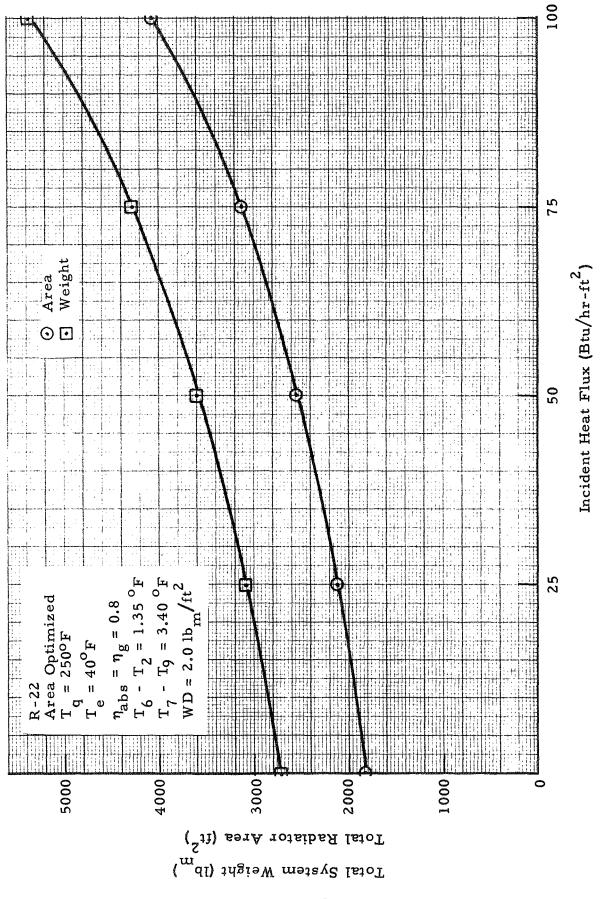
Fig. 31 - Effect of Varying Incident Heat Flux
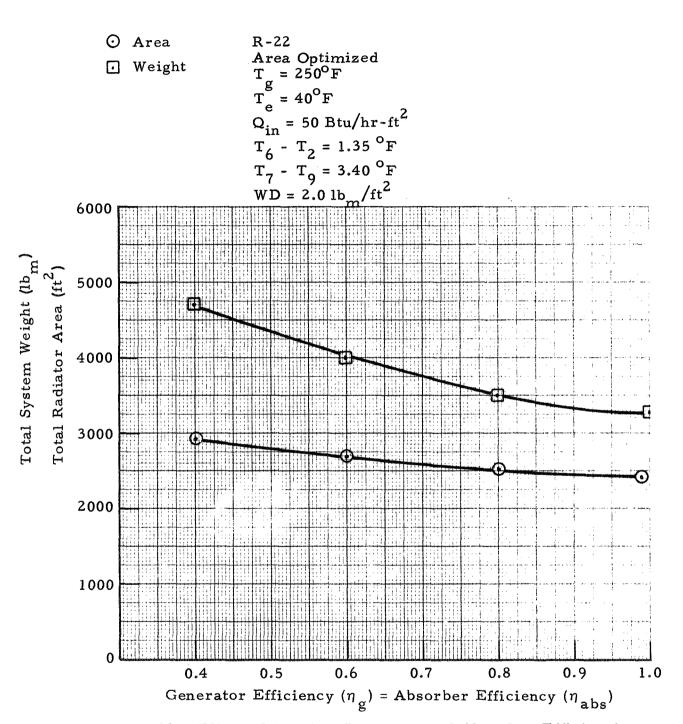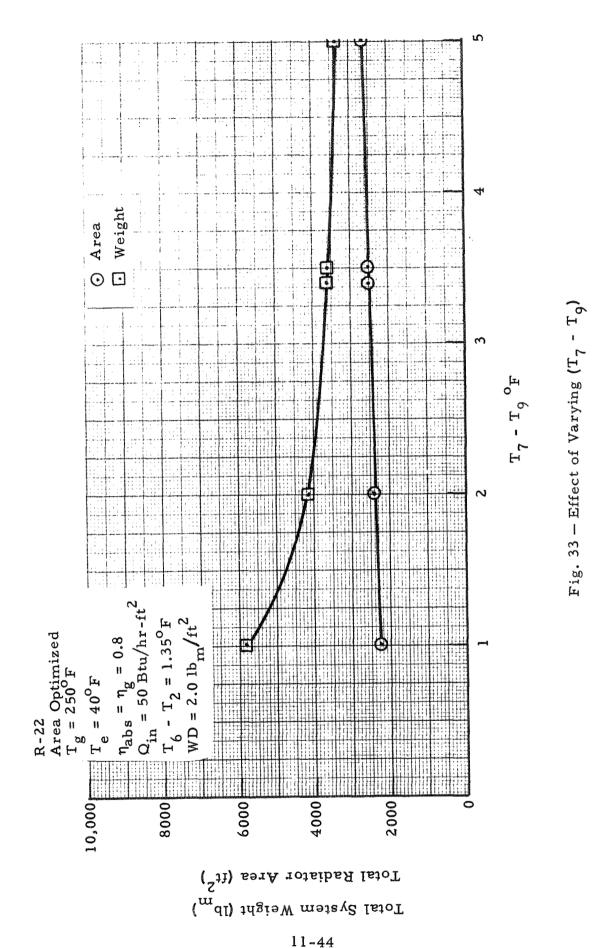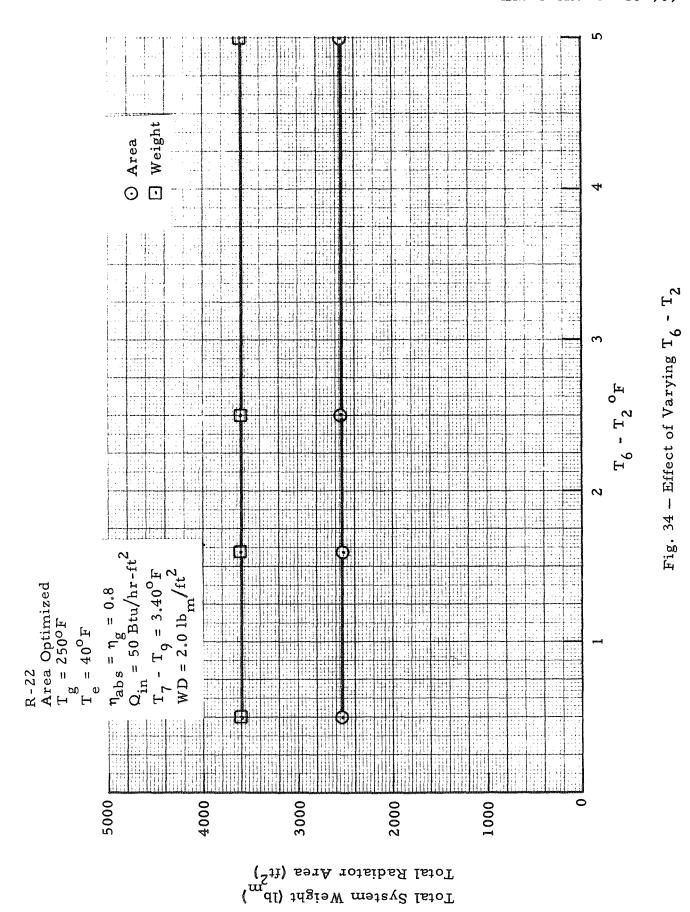
Fig. 32 — Effect of Varying Generator and Absorber Efficiencies
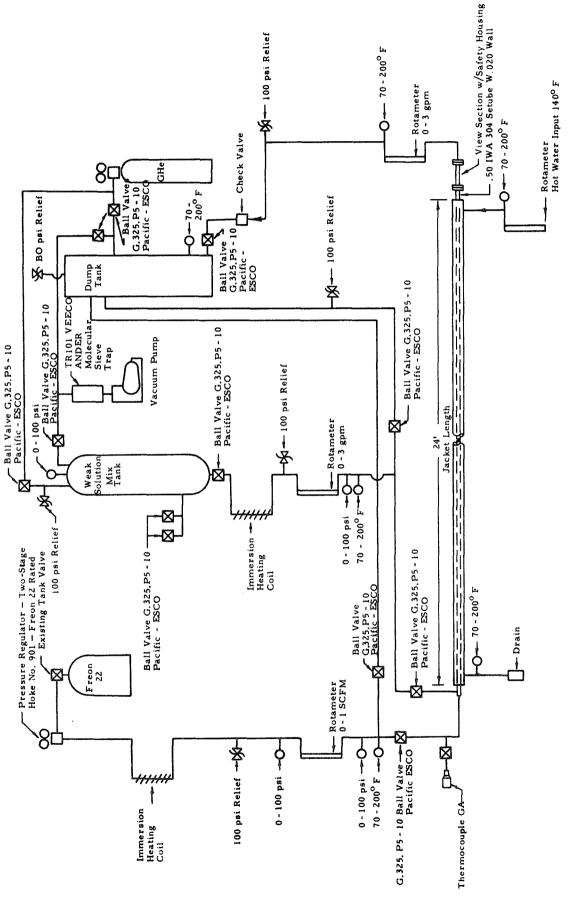
Fig. 33 — Effect of Varying $(T_7 - T_9)$

Fig. 34 — Effect of Varying $T_6 - T_2$

LOCKHEED - HUNTSVILLE RESEARCH & ENGINEERING CENTER

Fig. 35 – Detailed Flow Diagram of Absorber Test System
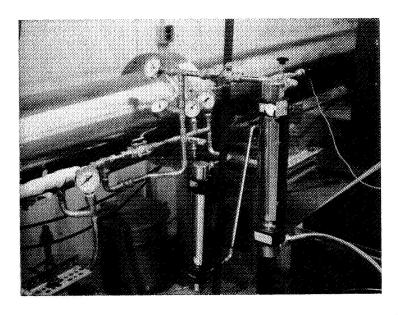
Fig. 36 - Absorber Inlet Section (Fig. 9, TP-3151)
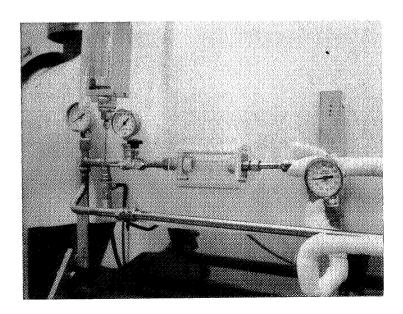
Fig. 37 - Absorber Exit (Fig. 3, TP-3151)

11-47

Fig. 38 - Absorption Refrigeration Cycle Test Schematic
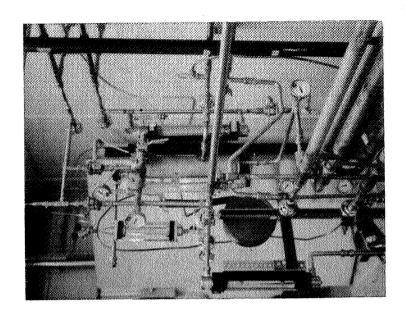
Fig. 39b - Separator Weak Liquid
Line to Recuperator
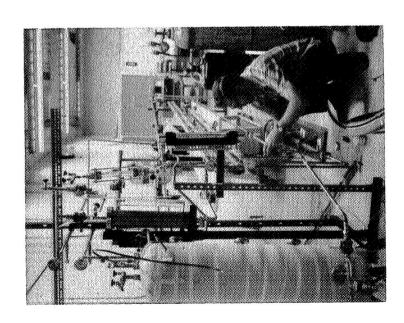
Fig. 39a - Assembly of Transfer
Line to Mix Tank

11-49
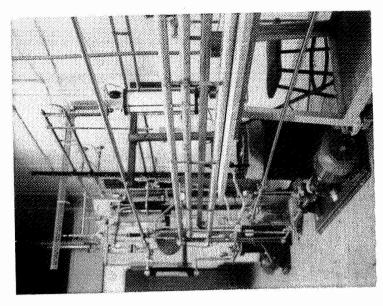
Fig. 39d - Recuperator Under Absorber
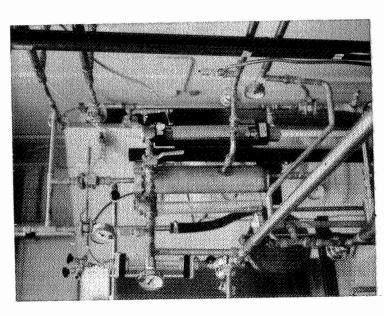
Fig. 39c - Strong Solution Entrance to Separator and Vapor Exit to Cooler
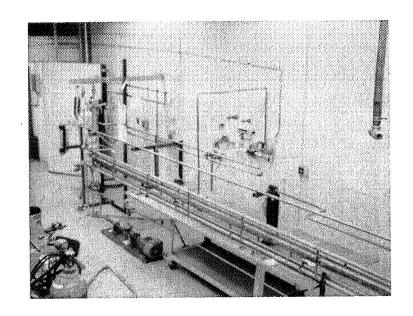
Fig. 39e - Vapor Cooler Above Generator
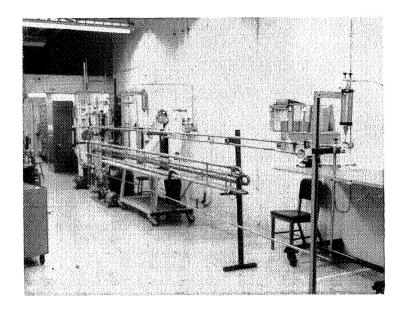
Fig. 39f - Absorber and Transfer Line to Pump

11-51
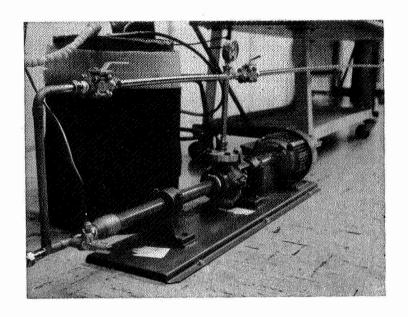
Fig. 39g - Pump
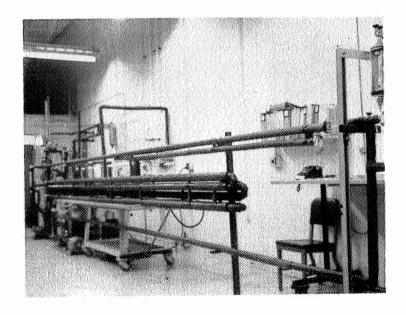
Fig. 39h - Test Loop with Insulations

11-52
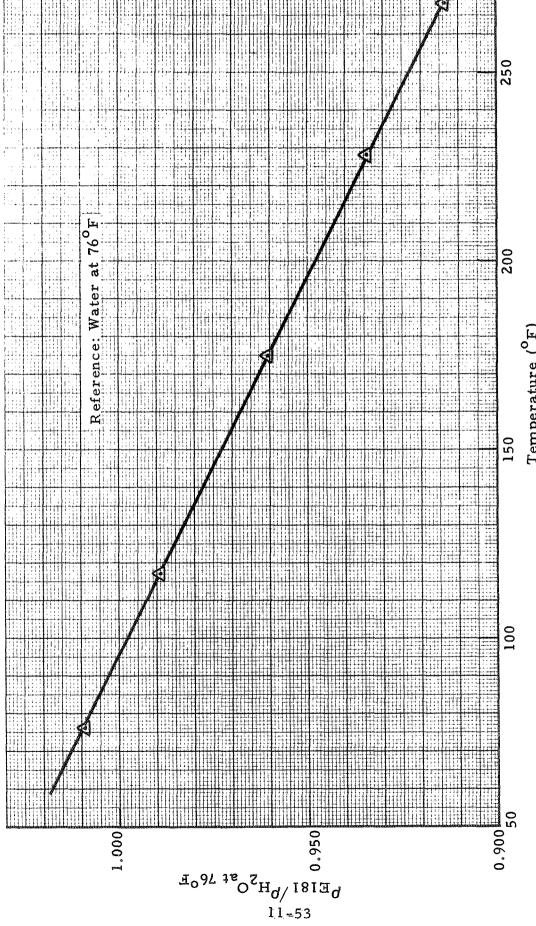
Fig. 40 - Temperature Dependence of Density of Ansul Polyether E-181 (DME-TEG)

LOCKHEED - HUNTSVILLE RESEARCH & ENGINEERING CENTER
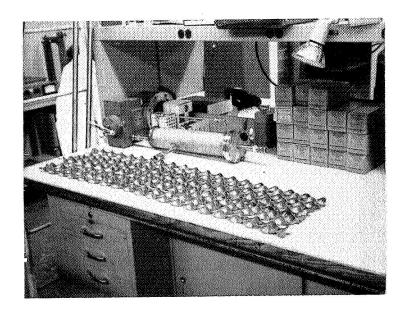
Fig. 41a - Twisted Tapes (Fig. 1, TP-3178)
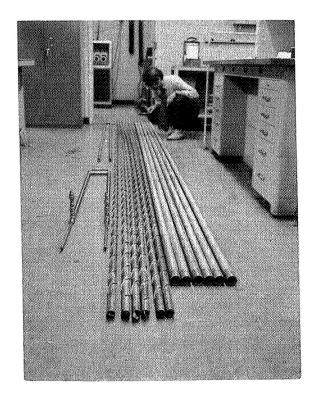
Fig. 41b - Inner and Outer Tubes of Recuperator (Fig. 3, TP-3178)

Vapor Exit

1-1/2

3

1/4 in. holes
1-in. apart on
0.011-in.
copper roll.

1/4-in. holes
1-in. apart in
Upper 6-in.

1/8-in. holes
1-in. apart in
the rest.

15

Copper roll
0.011-in.
wall.

$2\frac{5}{8}$

SS 304 Tube
4-in. o.d.
0.083-in. Wall

Deflector

18

6

View Glass

Liquid Exit

Fig. 42 - Liquid Vapor Separator

The ordinate is the power saved by use of a direct coupled motor-pump-motor package expressed as a percent of the electrical power demand without the hydraulic motor. The abscissa is percent of the pressure change across the pump that is lost in the strong and weak solution lines and component including the absorber but excluding the hydraulic motor.

Fig. 43 - Power Saved Versus Hydraulic Losses

Appendix A

R-22 AREA OPTIMIZED CYCLE COMPUTER PROGRAM
(VERSION 3)

```
C     R-22/DME-TEG                                                ONE   10
      DIMENSION T(8), HL(8), HVLO(8), HVHI(8), HAR(8)             ONE   20
      REAL LMTD1,LMTD2                                            ONE   30
      ICASE=0                                                     ONE   40
10    CONTINUE                                                    ONE   50
      ICASE=ICASE+1                                               ONE   60
C     TEMPERATURES IN DEGREES F                                  ONE   70
      READ (5,280) T(5),QIN,WD,ETAG,ETAA,DIF2,DIF7               ONE   80
      T(1)=40.0                                                   ONE   90
      T(3)=T(1)+0.3*(T(5)-T(1))                                  ONE  100
      T(6)=T(3)                                                   ONE  110
      T(2)=T(6)-DIF2                                              ONE  120
      T(7)=T(3)+DIF7                                              ONE  130
      T(4)=T(5)-T(7)+T(3)                                        ONE  140
      T(8)=T(6)                                                   ONE  150
      QEVAP=1990.92                                               ONE  160
      WRITE (6,290) ICASE                                         ONE  170
      WRITE (6,300)                                               ONE  180
      WRITE (6,310) QEVAP,QIN,WD,ETAG,ETAA                       ONE  190
      WRITE (6,320)                                               ONE  200
      WRITE (6,350) (T(I),I=1,8)                                 ONE  210
      DO 20 I=1,8                                                 ONE  220
20    T(I)=T(I)+460.                                              ONE  230
C     **   INITIAL DATA   **                                     ONE  240
      DEL3=0.5                                                    ONE  250
      DEL6=0.5                                                    ONE  260
      CONV=0.1                                                    ONE  270
C     REFRIGERANT-SOLVENT P-T-X DATA                             ONE  280
      D1=13.32                                                    ONE  290
      D2=4480.                                                    ONE  300
      D3=4970.                                                    ONE  310
      D4=4720.                                                    ONE  320
      D5=2.                                                       ONE  330
      FWR=86.5                                                    ONE  340
      FWA=222.2                                                   ONE  350
      RHOR=74.4                                                   ONE  360
      RHOA=62.                                                    ONE  370
      DELT4=1.0                                                   ONE  380
      DELT8=1.0                                                   ONE  390
      SPHTA=0.447                                                 ONE  400
      SPHTR=0.306                                                 ONE  410
C     EVAPORATOR COOLING CAPACITY IN BTU/MINUTE                  ONE  420
      PLO=EXP(12.530942-3675.966/T(1)-187262.0/T(1)**2)         ONE  430
C                                                                 ONE  440
C     **   BEGIN ITERATION LOOP   **                             ONE  450
C                                                                 ONE  460
      ITER=0                                                      ONE  470
      KT=1                                                        ONE  480
30    CONTINUE                                                    ONE  490
C     **   BEGIN OPTIMIZATION LOOP   **                          ONE  500
      DO 250 LOOP=1,2                                             ONE  510
      ICONV=0                                                     ONE  520
      ITER=ITER+1                                                 ONE  530
      IF (KT.NE.1) KT=2                                          ONE  540
      SIGN=1.0                                                    ONE  550
      JTER=0                                                      ONE  560
      IF (ITER.GT.30) GO TO 40                                   ONE  570
      GO TO 50                                                    ONE  580
```

```
   40 WRITE (6,330)                                                     ONE   590
      GO TO 10                                                          ONE   600
   50 CONTINUE                                                          ONE   610
      JTER=JTER+1                                                       ONE   620
C                                                                       ONE   630
      GO TO (60,70), LOOP                                               ONE   640
   60 T(3)=T(3)+DEL3*SIGN                                               ONE   650
      GO TO 80                                                          ONE   660
   70 T(6)=T(6)+DEL6*SIGN                                               ONE   670
   80 CONTINUE                                                          ONE   680
C                                                                       ONE   690
      PHI=EXP(12.530942-3675.966/T(6)-187262.0/T(6)**2)                ONE   700
      T(8)=T(6)                                                         ONE   710
      T(7)=T(3)+DIF7                                                    ONE   720
      T(4)=T(5)-T(7)+T(3)                                              ONE   730
      T(2)=T(6)-DIF2                                                    ONE   740
C     **   BEGIN WEIGHT CALCULATIONS   **                              ONE   750
      DO 90 N=1,7                                                       ONE   760
      TAU=T(N)-420.                                                     ONE   770
      HL(N)=SPHTR*TAU                                                   ONE   780
   90 CONTINUE                                                          ONE   790
      DO 100 N=1,2                                                      ONE   800
      HVLO(N)=.154*(T(N)-420.)+101.5-0.1*PLO*(T(N)/420.)**(-2.67)       ONE   810
  100 CONTINUE                                                          ONE   820
      HVHI(5)=.154*(T(5)-420.)+101.5-0.1*PHI*(T(5)/420.)**(-2.67)       ONE   830
      DO 110 N=3,7                                                      ONE   840
      HAB(N)=SPHTA*(T(N)-420.0)                                         ONE   850
  110 CONTINUE                                                          ONE   860
C     PERFORMANCE SEQUENCE                                              ONE   870
      WRL=QEVAP/(HVLO(1)-HL(1))                                         ONE   880
      HL(8)=HL(6)-HVLO(2)+HVLO(1)                                       ONE   890
  120 TAU=T(8)-420.                                                     ONE   900
      HAG=0.198*TAU+18.3E-4*TAU**2-14.7E-6*TAU**3+4.13E-8*TAU**4        ONE   910
      IF (HAG-HL(8)) 140,140,130                                        ONE   920
  130 T(8)=T(8)-DELT8                                                   ONE   930
      GO TO 120                                                         ONE   940
  140 T(8)=T(8)+DELT8/2.0                                               ONE   950
      WRV=WRL*(HL(8)-HL(1))/(HVLO(1)-HL(8))                            ONE   960
      A1=3.0-0.828E-2*T(3)+0.0413E-4*T(3)**2                          ONE   970
      A2=3.0-0.828E-2*T(5)+0.0413E-4*T(5)**2                          ONE   980
      XAE=A1+0.54*ALOG10(PLO)                                          ONE   990
      XGE=A2+0.54*ALOG10(PHI)                                          ONE  1000
      XA=(ETAG*XGE+ETAA/(1.-ETAA)*XAE)/(ETAG+ETAA/(1.-ETAA))          ONE  1010
      XG=(ETAA*XAE+ETAG/(1.-ETAG)*XGE)/(ETAA+ETAG/(1.-ETAG))          ONE  1020
      IF (XA-XG) 220,220,150                                           ONE  1030
  150 WRC=(WRL+WRV)*(1.0-XA)*XG/(XA-XG)                                ONE  1040
      WAB=FWA*WRC*(1.0-XG)/(FWR*XG)                                    ONE  1050
C     Q VALUES                                                         ONE  1060
      CALL HEAT (T(7),XG,DELHM7)                                       ONE  1070
      QMIX7=(WRC+WAB)*DELHM7                                           ONE  1080
      CALL HEAT (T(3),XA,DELHM3)                                       ONE  1090
      QMIX3=(WRL+WRV+WRC+WAB)*DELHM3                                   ONE  1100
      QABS=(WRL+WRV)*HVLO(2)+WRC*HL(7)-(WRL+WRV+WRC)*HL(3)+WAB*(HAB(7)-HONE 1110
     1AB(3))+QMIX3-QMIX7                                               ONE  1120
      QREC=WRC*(HL(5)-HL(7))+WAB*(HAB(5)-HAB(7))                       ONE  1130
  160 HAB(4)=HAB(3)+(QREC-(WRL+WRV+WRC)*(HL(4)-HL(3)))/WAB            ONE  1140
      Y=HAB(4)/SPHTA+420.0                                             ONE  1150
      IF (Y-T(4)) 170,180,180                                          ONE  1160
```

A-2

```
  170 T(4)=T(4)-DELT4                                                    ONE 1170
      TAU=T(4)-420.                                                      ONE 1180
      HL(4)=SPHTD*TAU                                                    ONE 1190
      GO TO 160                                                          ONE 1200
  180 T(4)=0.5*(T(4)+Y)                                                  ONE 1210
      CALL HEAT (T(4),XA,DELHM4)                                         ONE 1220
      QMIX4=(WRL+WRV+WRC+WAB)*DELHM4                                     ONE 1230
      CALL HEAT (T(5),XG,DELHM5)                                         ONE 1240
      QMIX5=(WRC+WAB)*DELHM5                                             ONE 1250
      QGEN=(WRL+WRV)*HVHI(5)+WRC*HL(5)-(WRL+WRV+WRC)*HL(4)+WAB*(HAB(5)-HONE 1260
     1AB(4))+QMIX4-QMIX5                                                 ONE 1270
      QCOND=(WRL+WRV)*(HVHI(5)-HL(6))                                    ONE 1280
      QSUB=(WRL+WRV)*(HVLO(2)-HVLO(1))                                   ONE 1290
      QPUMP=((WRL+WRV+WRC)/RHOR+WAB/RHOA)*0.185*(PHI-PLO)                ONE 1300
C     SYSTEM MASSES PER UNIT KW COOLING CAPACITY                        ONE 1310
      WF=55.2                                                            ONE 1320
C     ABSORBER RADIATING FROM BOTH SIDES                                ONE 1330
      AABS=(60.0*QABS)/(0.15426E-08*T(3)**4-QIN)                        ONE 1340
      WA=WD*AABS/2.0                                                     ONE 1350
      RHOE=(WRL+WRV+WRC+WAB)/((WAB/63.11)+(WRL+WRV+WRC)/76.773)          ONE 1360
      WP=(8.72*(WRL+WRC+WRV+WAB)*(PHI-PLO)/RHOE)**0.546                  ONE 1370
      WPP=0.0                                                            ONE 1380
      LMTD1=(T(5)-T(4)+T(3)-T(7))/ALOG((T(5)-T(4))/(T(7)-T(3)))          ONE 1390
      LMTD2=(T(6)-T(2)+T(1)-T(8))/ALOG((T(6)-T(2))/(T(8)-T(1)))          ONE 1400
      WREC=50.3*(60.0*QREC/(25200.0*LMTD1))**0.882                       ONE 1410
      WG=175.35*QGEN/QEVAP                                               ONE 1420
C     CONDENSER RADIATING FROM BOTH SIDES                               ONE 1430
      ACOND=(60.0*QCOND)/(0.15426E-08*T(6)**4-QIN)                      ONE 1440
      WC=WD*ACOND/2.0                                                    ONE 1450
      WSUB=28.3*(60.0*QSUB/(3100.0*LMTD2))**0.882                       ONE 1460
      WLF=0.264*WF                                                       ONE 1470
      WLREC=0.0234*RHOA*WREC                                             ONE 1480
      WLSUB=0.645*WSUB*(RHOR/74.4)                                       ONE 1490
      WTOT=WA+WP+WREC+WC+WSUB+WLREC+WLSUB                                ONE 1500
      TARAD=AABS+ACOND                                                   ONE 1510
      IF (ICONV.GT.0) GO TO 220                                         ONE 1520
C     **   END OF WEIGHT CALCULATIONS  **                               ONE 1530
C     **   CHECK FOR OPTIMIZATION  **                                   ONE 1540
      IF (KT.NE.1) GO TO 190                                            ONE 1550
      ARAD=TARAD                                                         ONE 1560
      KT=2                                                               ONE 1570
      GO TO 50                                                           ONE 1580
  190 IF (TARAD.GT.ARAD) GO TO 200                                      ONE 1590
      ARAD=TARAD                                                         ONE 1600
      IF (SIGN.EQ.-2.) SIGN=-1.                                         ONE 1610
      KT=3                                                               ONE 1620
      GO TO 50                                                          ONE 1630
  200 IF (KT.EQ.3) GO TO 210                                           ONE 1640
      KT=3                                                               ONE 1650
      SIGN=-2.0                                                         ONE 1660
      GO TO 50                                                          ONE 1670
  210 CONTINUE                                                          ONE 1680
      IF (SIGN.EQ.-2.) SIGN=-1.0                                       ONE 1690
      SIGN=-SIGN                                                         ONE 1700
      ICONV=1                                                           ONE 1710
      GO TO 50                                                          ONE 1720
C     **  OUTPUT SECTION  **                                            ONE 1730
  220 ARAD=TARAD                                                        ONE 1740
```

```
      WRITE (6,340) ITER,JTER                                        ONE 1750
      DO 230 I=1,8                                                   ONE 1760
230   T(I)=T(I)-460.0                                               ONE 1770
      WRITE (6,350) (T(I),I=1,8)                                     ONE 1780
      DO 240 I=1,8                                                   ONE 1790
240   T(I)=T(I)+460.                                                ONE 1800
      WRITE (6,360) DIF2,DIF7                                        ONE 1810
      WRITE (6,370) QEVAP,QABS,QPUMP,QREC,QGEN,QCOND,QSUB            ONE 1820
      WRITE (6,380) WE,WA,WP,WPP,WREC,WG,WC,WSUB                     ONE 1830
      WRITE (6,390) XA,XG                                            ONE 1840
      WRITE (6,400) WRL,WRV,WRC,WAB                                  ONE 1850
      WRITE (6,410) WLE,WLREC,WLSUB                                  ONE 1860
      WRITE (6,420) PHI,PLO                                          ONE 1870
      WRITE (6,430) (HL(I),I=1,8)                                    ONE 1880
      WRITE (6,440) HVLO(1),HVLO(2),HVHI(5)                          ONE 1890
      WRITE (6,450) (HAB(I),I=3,7)                                   ONE 1900
      WRITE (6,460) XAE,XGE,LMTD1,LMTD2                              ONE 1910
      WRITE (6,470) AABS                                             ONE 1920
      WRITE (6,480) ACOND                                           ONE 1930
      WRITE (6,490) TARAD                                           ONE 1940
      WRITE (6,500) WTOT                                            ONE 1950
      WRITE (6,510) QMIX3,QMIX4,QMIX5,QMIX7                          ONE 1960
250   CONTINUE                                                      ONE 1970
C     **  END OF OPTIMIZATION LOOP  **                              ONE 1980
C     **  CHECK FOR CONVERGENCE BASED ON T(6)  **                   ONE 1990
      IF (ITER.EQ.2) GO TO 260                                      ONE 2000
      DT=ABS(T6S-T(6))                                              ONE 2010
      IF (DT.LT.CONV) GO TO 270                                     ONE 2020
260   T6S=T(6)                                                      ONE 2030
      GO TO 30                                                       ONE 2040
C     **  END OF ITERATION LOOP  **                                 ONE 2050
270   WRITE (6,520) ITER                                            ONE 2060
      GO TO 10                                                       ONE 2070
C                                                                    ONE 2080
280   FORMAT (8F10.0)                                               ONE 2090
290   FORMAT (32H1I N P U T    D A T A    CASE NO.,I5///)           ONE 2100
300   FORMAT (46H0THE REFRIGERATOR FLUIDS ARE R-22 AND DME-TEG ///) ONE 2110
310   FORMAT (7H0QEVAP=,E12.5,10X,4HQIN=,E12.5,10X,3HWD=,E12.5,10X,5HETAONE 2120
     1G=,E12.5,10X,5HETAA=,E12.5///)                                ONE 2130
320   FORMAT (34H0TOTAL RADIATOR AREA IS OPTIMIZED )                ONE 2140
330   FORMAT (47H0THE SOLUTION DIDNOT CONVERGE IN 30 ITERATIONS )   ONE 2150
340   FORMAT (1H1//23H O U T P U T   D A T A ,13HITERATION NO.I4,10X,5HJONE 2160
     1TER=I4///)                                                    ONE 2170
350   FORMAT (5X,9HT1 (EVAP),8X,2HT2,11X,8HT3 (ABS),8X,2HT4,11X,8HT5 (GEONE 2180
     1N),8X,9HT6 (COND),8X,2HT7,12X,2HT8/8E15.6)                    ONE 2190
360   FORMAT (1H0,5X,4HDIF2,13X,4HDIF7/2E15.6)                      ONE 2200
370   FORMAT (1H0,7X,5HQEVAP,10X,4HQABS,10X,5HQPUMP,10X,4HQREC,10X,4HQGEONE 2210
     1N,10X,5HQCOND,10X,4HQSUB/7E15.6)                              ONE 2220
380   FORMAT (1H0,7X,2HWE,12X,2HWA,12X,2HWP,12X,3HWPP,13X,4HWREC,12X,2HWONE 2230
     1G,12X,2HWC,12X,4HWSUB/8E15.6)                                 ONE 2240
390   FORMAT (1H0,7X,2HXA,12X,2HXG/2E15.6)                          ONE 2250
400   FORMAT (1H0,7X,3HWRL,11X,3HWRV,12X,3HWRC,12X,3HWAB/4E15.6)    ONE 2260
410   FORMAT (1H0,7X,3HWLE,11X,5HWLREC,9X,5HWLSUB/3E15.6)           ONE 2270
420   FORMAT (1H0,7X,4HP HI,11X,4HP LO/2E15.6)                      ONE 2280
430   FORMAT (1H0,7X,5HHL(1),10X,5HHL(2),10X,5HHL(3),10X,5HHL(4),10X,5HHONE 2290
     1L(5),10X,5HHL(6),10X,5HHL(7),10X,5HHL(8)/8E15.6)             ONE 2300
440   FORMAT (1H0,7X,7HHVLO(1),8X,7HHVLO(2),8X,7HHVHI(5)/3E15.6)    ONE 2310
450   FORMAT (1H0,7X,6HHAB(3),9X,6HHAB(4),9X,6HHAB(5),9X,6HHAB(6),9X,6HHONE 2320
```

```
       1AP(7)/5E15.6)                                                        ONE  2330
460 FORMAT (1H0,7X,3HXAF,12X,3HXGE,12X,5HLMTD1,10X,5HLMTD2/4E15.6//)         ONE  2340
470 FORMAT (31H0THE ABSORBER RADIATOR AREA IS F15.6//)                       ONE  2350
480 FORMAT (32H0THE CONDENSER RADIATOR AREA IS E15.6//)                      ONE  2360
490 FORMAT (28H0THE TOTAL RADIATOR AREA IS E15.6//)                          ONE  2370
500 FORMAT (73H0THE TOTAL REFRIGERATOR WEIGHT EXCLUDING THE EVAPORATORONE    ONE  2380
       1 AND GENERATOR IS F15.6///)                                          ONE  2390
510 FORMAT (7HQMIX3=,E15.6,10X,6HQMIX4=,E15.6,10X,6HQMIX5=,E15.6,10X,ONE     ONE  2400
       16HQMIX7=,E15.6)                                                      ONE  2410
520 FORMAT (22H1SOLUTION CONVERGED IN,I5,3X,10HITERATIONS)                   ONE  2420
    END                                                                      ONE  2430
```

```
    SUBROUTINE HEAT (T,XR,DELHM)                                             TWO   10
    REAL MWAVG                                                              TWO   20
    TOL=.001                                                                TWO   30
    F=3.0                                                                   TWO   40
    Z=0.0                                                                   TWO   50
    DELHR=4100.0                                                            TWO   60
    TKELVN=T/1.8                                                            TWO   70
    XK=EXP((2060.0/TKELVN)-6.77)                                            TWO   80
 10 DELHM=(DELHR*((F*XK)/(1.+XK))*XR*(1.-XR))/(XR+F*(1.-XR)-Z)              TWO   90
    ZOLD=Z                                                                  TWO  100
    Z=DELHM/DELHR                                                           TWO  110
    CHECK=ABS(Z-ZOLD)                                                       TWO  120
    IF (CHECK.LT.TOL) GO TO 20                                              TWO  130
    GO TO 10                                                                TWO  140
 20 MWAVG=XR*86.5+(1.-XR)*222.2                                             TWO  150
    DELHM=1.8*DELHM/MWAVG                                                   TWO  160
    RETURN                                                                  TWO  170
    END                                                                     TWO  180
```

Appendix B

EXPERIMENTAL TESTS ON FLUID PROPERTIES

Appendix B

In order to determine the flow parameters (Reynolds number and Prandtl number, etc) in the design of various heat transfer surfaces, as well as the transfer lines, it is necessary to have the fluid properties like density, specific heat, viscosity, thermal conductivity, etc. The fluid properties of R-22 are readily available, but only limited data on DME-TEG (Ansul polyether E-181) are known.

For the immediate need of the present investigation, the specific gravity of the Ansul Polyether E-181 (DME-TEG) was determined between room temperature and $268^{\circ}F$ in an inert atmosphere oven by a volume-gravimetric technique. The oven was purged with dry nitrogen to minimize any tendency to form peroxides. Two parallel measurements were made at each randomly selected temperature and the comparison of the results as given in Table 6 indicated no trend toward systematic errors.

A fresh supply of E-181 was placed in two (25 ml) Pyrex pycnometer bottles prior to each run. The bottles, when filled and weighed at the laboratory temperature of $76^{\circ}F$, were each placed in an aluminum cup and transferred to the oven. Expansion due to temperature elevation forced an excess amount of E-181 out of the capillary in the ground glass stopper and into the cups. After equilibrium temperature is reached (1-2 hours), the specimens were removed and the excess external material spilled on the side of the bottle was wiped off. The values of specific gravity of the E-181 at various temperatures were plotted in Fig. 40.

Evaporation of the internally contained E-181 is neglected due to the low vapor pressure and the small exit port of the capillary. Thermal expansion of the Pyrex bottles is also neglected.

B-1

The effect of R-22 and DME-TEG solution on several materials was examined by immersion of brass, viton, solder and silver solder. The solution was at a refrigerant concentration of .54 and was maintained at $150^{\circ}F$ and 200 psia for 116 hrs. No appreciable decomposition of R-22 nor adverse effect on the sample materials were observed.

Appendix C

ABSORBER DESIGN

Appendix C

The various design concepts for gravity independent absorbers are given in Table 7. In the present investigation, concept A was chosen for its simplicity. The heat flux in the absorber is (at 1/53rd scale) 45.6 BTU/min. An overall heat transfer coefficient of 200 BTU/Hr-Ft^2-$^\circ$F is assumed for a counterflow concentric-tube type absorber with cooling water flowing in the outer jacket to simulate a heat sink as space radiator. The outer tube has an 1-inch O.D. with .049-inch wall and the inner tube of 0.5-inch O.D. with .020-inch wall. If the average temperature difference between the fluid is 6.5°F, the length of the absorber is 16 ft. In the present test, a cooling length of 23 ft. is used.

The weak solution enters the mixing section through a jet with four (4) copper wires of 0.013-inch diameter placed criss-cross the opening of the jet. The effective opening is 0.4 x 10^{-4} Ft^2 and a pressure head of 30 to 35 psi is provided upstream of the jet to yield a high velocity spray at the exit.

Temperatures, pressures and flow rates of the fluids entering and leaving the absorber are measured by standard bimetallic dial thermometers, pressure gauges and flow rotameters. The concentrations of the weak and strong solutions are determined by the failure pressure of the liquid withdrawn from the flow line into the samplers.

LOCKHEED · HUNTSVILLE RESEARCH & ENGINEERING CENTER

Appendix D

PROCEDURES OF PRELIMINARY TEST ON THE ABSORBER

Appendix D

Preparation

After a thorough cleaning of all sub-assemblies with hot water for the removal of silver solder flux and other contaminants, the assembled system was purged with dry nitrogen and with helium gas. After purging, a vacuum check was initiated on all assembled components up to the regulator valve outputs on the helium and R-22 tanks. Following the vacuum integrity check a pressure test to the 240 psia level was conducted on all rated components in the assembled form. Because of the hazardous aspects of the working fluid, a zero leak rate was achieved and maintained throughout the tests.

Operations

Before the test run, the weak solution in the mixing tank was stirred and heated to $145^\circ F$ at about 55 psig. The tank was pressurized by helium gas to 110 psig just before and during the test run.

In order to maintain the R-22 vapor flow rate, the R-22 containers were heated by electrical heating tapes wrapped around the lower portion of the containers. The test run was ready to begin when the vapor pressure in the R-22 supply manifold reached 300 psi which is just below the setting of the relief valve on the R-22 containers.

At the beginning of the test run, the weak solution was introduced to the absorber at the scaled-down design flow rate of 8.97 lb/min at $142^\circ F$ with the absorber exit pressure maintained at 82.9 psia. The R-22 vapor was then introduced into the absorber at 0.503 lb/min, $109^\circ F$ and 83.9 psia.

D-1

(It was at this stage that the flow rates of the weak solution and R-22 vapor, as well as the absorber exit pressure fluctuate.) The weak solution inlet valve, R-22 vapor inlet valve and the discharge valve to the dump tank were adjusted simultaneously to obtain the design flow rates and the absorber exit pressure.

As soon as the design flow rates and the absorber exit pressure were obtained, the view section located at the absorber exit showed clear liquid flow instead of bubble flow or stratified flow which appeared during the flow adjustment period. The test run was terminated immediately due to the limited capacity of the fluid supply. The liquid samples were taken and the fluid properties were read at the completion of the test run.

One additional test was run under identical conditions for motion picture data.

D-2

Appendix E

RECUPERATOR DESIGN

Appendix E

Based on the results of the computer parametric studies, the recuperator has the highest heat flux requirement among all the heat transfer components. In order to increase the cycle efficiency, the recuperator flow parameters are specified as follows (scaled down to 1/53rd).

Cold fluid: 9.475 lb_m/min of strong solution to be heated from 138.5°F to 242°F at 247.7 psia.

Hot fluid: 8.972 lb_m/min of weak solution to be cooled from 250°F to 141°F at 247.7 psia.

The heat rate as calculated from the values of enthalpy given in Table 2 is 398 Btu/min. Since $Q = \dot{m}\, C_p\, \Delta T$, the average values[*] of the specific heat assumed for weak and strong solutions are

$$\overline{C}_{p_W} = 0.42 \ \text{Btu}/lb_m \,°F$$

and

$$\overline{C}_{p_S} = .406 \ \text{Btu}/lb_m \,°F.$$

If a counterflow concentric-tube type arrangement is used, the logarithmic temperature difference is $\Delta t_m = 5.37°F$. Since $Q = US\,\Delta t_m$, this yields

$$US = Q/\Delta tm = 74.1 \ \text{Btu/min} \ °F$$

The fluid capacity rate of the weak and strong solutions are

$$\overset{\circ}{C}_W = \dot{m}_W\, \overline{C}_{p_W} = 3.77 \ \text{Btu/min} \ °F$$

$$\overset{\circ}{C}_S = \dot{m}_S\, \overline{C}_{p_S} = 3.85 \ \text{Btu/min} \ °F$$

---

[*]See Appendix K for nomenclature.

E-1

Hence, the number of transfer unit is

$$NTU = \frac{US}{\dot{C}_{min}} = 19.65$$

This is a very high value due to the high effectiveness assumed for this recuperator. The effectiveness is

$$\epsilon = \frac{250 - 141.9}{250 - 138.5} = 97.0\%$$

The ratio of the fluid capacity rates is

$$\frac{\dot{C}_w}{\dot{C}_s} = 0.979$$

From Ref. 29, Table 2-1, it is also seen that $\epsilon = 0.970$ required that NTU $\approx$ 20. In order to determine the size of the recuperator, it is necessary to calculate the overall heat transfer coefficient.

If a counterflow concentric-tube type heat exchanger is considered with tubes of 1.625-inch O.D., 0.049 inch wall and 1.125 inch O.D. with 0.050-inch wall, the flow areas are 0.577×10^{-2} ft^2 and 0.572×10^{-2} ft^2, respectively for annular and inner tube side. The larger tube diameter provided larger heat transfer area, lower pressure drop but lower heat transfer coefficients. These are calculated as follows if the weak solution is assumed to flow on the inner tube side and the strong solution on the annular side. (In the final design the strong solution is flowing in the inner tube with twisted tapes. However, the sizing of the component is not significantly affected.)

Inner Tube Side - Weak Solution

$$\rho_w = 55.66 \ Lb/Ft^3$$

$$V_w = 0.251 \ Ft/Sec$$

$$\mu = 2.2 \ C.P. = 4.61 \times 10^{-5} \ lb_f/sec/ft^2$$

$$\overline{C}_{pw} = .42 \ \text{Btu-lb-}^{\circ}\text{F}$$

$$k_w \simeq 0.11 \ \text{Btu/hr-ft-}^{\circ}\text{F}$$

This yields the following flow parameters

$$Re_w = \frac{\rho_w V_w D}{\mu_w} = 1100$$

$$Pr_w = \frac{\overline{C}_{pw} \mu_w}{k_w} = 20.5$$

This indicates that the inner tube side flow is laminar. Since the tube wall temperature varies from inlet to exit, the correlation for a fully developed laminar flow inside a tube with constant heat flux is used to yield

$$h_w = \frac{k_w}{D} \cdot 4.36 = 4.1 \ \text{Btu/hr-ft}^2\text{-}^{\circ}\text{F}$$

This is too low and requires extremely long tubes.

If 0.50 - inch tube is used as in the absorber, the Reynolds number is about 3350 and the heat transfer coefficient of a turbulent flow inside a tube is (Ref. 30)

$$h_w = 0.0265 \frac{k_w}{D} \ Re^{0.8} \ Pr^{0.3} = 40 \ \text{Btu/hr-ft}^2\text{-}^{\circ}\text{F}$$

However, this increase in h_w is compromised by the decrease of the tube perimeter and the length of tube for the required heat transfer surface becomes even longer.

Annulus Side - Strong Solution

$$\rho_s = 56.5 \ \text{lb/ft}^3$$

$$V_s = 0.41 \ \text{ft/sec}$$

$$\mu_s = 4.85 \times 10^{-5} \ \text{lb}_f\text{-sec/ft}^3$$

$$\overline{C}_{p_s} = 0.397 \ \text{Btu/lb}_m\text{-}^{\circ}\text{F}$$

E-3

$$k_s = 0.12 \text{ Btu/hr-ft-}^\circ\text{F}$$

$$D_h = 4r_h = 2.69 \times 10^{-2} \text{ ft.}$$

This yields the following flow parameter

$$Re_s = 420$$

Neglecting natural convection, the film coefficient for laminar flow in annuli space is estimated for each length of 20 ft (Ref. 31).

$$h_s \sim \frac{k}{D} \left(\frac{D_o}{D_i}\right)^{0.8} \left(\frac{\dot{m} \, c_p}{kL}\right)^{0.45} = 40.8 \text{ Btu/hr-ft}^2\text{-}^\circ\text{F}$$

In the case where the heat transfer coefficient is lower on the annulus side, external fins are usually used. In the present case, where the dominant resistance to the heat flow is on the tube side, the performance of the recuperator may be increased by placing a twisted tape inside the tube. First, the fluid velocity passing the wall of the tube is greater for the same mass flow. Secondly, the wall of the tube is concave with respect to the direction of fluid flow. Both of these yield a larger heat transfer coefficient as shown in Ref. 32. Finally, a centrifugal force field is set up by the rotation of the fluid in a swirl flow. This has a favorable convection effect if the heat flow is directed inward as cold fluid of higher density will be flung outward from the center of the tube.

In order to design a recuperator for the present test loop without excessive length, the strong solution will pass through the inner tube with twisted tape brazed to the wall to increase the heat transfer efficiency from the "fin-effects". Twisted tapes were made from 1.05-in. wide soft copper strips of 0.065 in. thick and 48 in. long. The tapes were twisted in a horizontal position by clamping both ends on bench vises with one end free to rotate by use of a roller thrust bearing. The tape was first stretched to create some initial stress and then twisted 360 deg per 5.01 $\pm$ 0.01 in. to cause yield stress in the strip. These strips were then unloaded and annealed by heating to red heat before being quenched in water. After being pickled

in nitric acid to remove scales and then polished with a motor-driven wire brush, the 4-ft. tapes were soldered together to form six 20-feet long continuous tapes of 1.020 ± 0.003-in. wide. These were placed inside the 1.125-in. O.D. (0.050 - in. wall) copper inner tubes of the recuperator. Soft 0.125-in. O.D. copper tubings were wound around the outside of these inner tubes at 360 deg per 6-in. These were then placed inside the 1.625-in. O.D. (0.049-9n. wall) stainless steel outer tubing to form the main body of the recuperator.

Fig. 41a shows the twisted tapes and Fig. 41b shows the inner and outer tubes.

Appendix F

GENERATOR DESIGN

Appendix F

The various design concepts for gravity independent generators are given in Table 8 and the methods of heat addition to the generator in Table 9. In the present investigation, simple straight tubes with electrical heating are used.

The generator temperature is limited to 250°F to assume the safety of the operation. The heat input required (scaled down to 1-53d) is 55.9 Btu/min or 0.99 KW. Stainless steel tubes of 1-inch O.D. and 0.049-inch wall are used. The liquid properties at the inlet of the generator are[*]

$$\rho_L = 48.7 \text{ lb/ft}^3$$

$$V_L = 0.718 \text{ ft/sec}$$

$$\mu_L = 1.7 \text{ C.P.} = 3.6 \times 10^{-5} \text{ lb}_f\text{-sec/ft}^2$$

$$k_L = 0.15 \text{ Btu/hr-ft-}^{\circ}\text{F}$$

$$\overline{C}_p = 0.43 \text{ Btu/lb}_m\text{-}^{\circ}\text{F}$$

Based on above, the average heat transfer coefficint of liquid on the hot wall is (Ref. 30)

$$h_o = .0243 \frac{k}{D} Re^{0.8} Pr^{0.4} = 36 \text{ Btu/hr-ft}^2\text{-}^{\circ}\text{F}$$

Based on this value of heat transfer coefficient of single-phase flow, the relationship proposed in Ref. 33 can be used to calculate the heat transfer coefficient in two-phase flow

$$\frac{h}{h_o} = 17.5 \; B_o^{0.2} \; (x_{tt})^{-0.167}$$

[*] See Appendix K for nomenclature.

where

$$B_o = \text{boiling number} = q/rG$$

$$r = \text{latent heat of vaporization}$$

$$G = \text{mass velocity of fluid}$$

$$x_{tt} = \text{Lockhart \& Martinelli parameter}$$

$$= \left(\frac{1-x}{x}\right)^{0.9} \left(\frac{\rho_g}{\rho_\ell}\right)^{0.5} \left(\frac{\mu_\ell}{\mu_g}\right)^{0.1}$$

$$x = \text{weight fraction of vapor in liquid}$$

This yields $h = 80$ Btu/hr-ft^2 - $^\circ$F. The generator tubes are heated by Cole-Parmer heating tapes with maximum total input wattage of 3.73 kW (212 Btu/min.). To improve the performance, twisted tapes may be inserted into the tube and an average overall heat transfer coefficient of 200 Btu/hr-ft^2-$^\circ$F can be assumed (Ref. 34). If a logarithmic mean temperature difference of 10°F is assumed between the hot wall and the bulk of the flow, the heating length required will be

$$L = \frac{55.9 \times 60 \times 12}{200 \times \pi \times .902 \times 10} = 8 \text{ ft.}$$

For the present test, two lengths of 10-ft. tubes as shown in the background of Figure 41b were used for the generator without twisted tapes.

Appendix G

SEPARATOR DESIGN

Appendix G

Various design concepts for gravity independent liquid-vapor separators are given in Table 10. For the present investigation, a simple vortex-gravity type based on the design in Figure 42 was fabricated.

LOCKHEED · HUNTSVILLE RESEARCH & ENGINEERING CENTER

Appendix H

COOLER DESIGN

Appendix H

The R-22 vapor from the separator will be cooled from $250°F$ to $145°F$ at 247.7 psia (see Table 2 and Fig. 20). The amount of heat to be rejected to the cooling water is 9.79 Btu/min. For the present test, a concentric tube type cooler will be used with R-22 vapor flowing inside a 0.5-inch copper tubing of 0.035-inch wall and water flowing inside the annuli formed with a 1.0-inch stainless steel tubing of 0.049-inch wall. The mean fluid properties on the inner tube side are[*]

$$\rho_g = 3.5 \text{ lb/ft}^3$$

$$V = 2.4 \text{ ft/sec}$$

$$\mu = .0154 \text{ c.p.} = 3.22 \times 10^{-7} \text{ lb}_f/\text{sec/ft}^2$$

$$\overline{C}_p = 0.21 \text{ Btu/lb-}°F$$

$$k = .0083 \text{ Btu/hr-ft-}°F$$

These yield the flow parameters of

$$Pr = 2.26$$

$$Re = 2.91 \times 10^4$$

The heat transfer coefficient on the inner tube side is (Ref.30).

$$h = 0.0243 \frac{k}{D} Re^{0.8} Pr^{0.4} = 290 \text{ Btu/hr-ft}^2-°F$$

On the annulus side, the average water properties are

$$\rho_w = 61.6 \text{ lb/ft}^3$$

$$V_w = 0.294 \text{ ft/sec}$$

---

[*]See Appendix K for nomenclature

$$\mu_w = 11.8 \times 10^{-6} \text{ lb}_f\text{-sec}/\text{ft}^2$$

$$Pr \simeq 3.68$$

$$d_h = 4 \ \frac{\text{flow area}}{\text{wetted parameter}} = 0.334 \text{ ft}.$$

These yield the Reynolds number of 1.6×10^4. The mean heat transfer coefficient of turbulent water flow on the shell side is (Ref. 31).

$$h_w = 0.023 \ C_p G \ Re^{-.2} \ Pr^{-2/3} \ \varphi$$

where

$$\varphi = 0.87 \ \left(\frac{.902}{.46}\right)^{0.53} = 1.245$$

These yield a h_w of 179 $\text{Btu}/\text{hr-ft}^2\text{-}^\circ\text{F}$.

For .035-inch copper wall and $k \simeq 200 \text{ Btu}/\text{hr-ft-}^\circ\text{F}$, the mean overall heat transfer coefficient is estimated to be

$$U = 110 \text{ Btu}/\text{hr-ft}^2\text{-}^\circ\text{F}$$

The mean logarithmic temperature difference is 25°F. The length of tube is therefore

$$L = \frac{9.79 \times 60 \times 12}{\pi \times 0.5 \times 110 \times 25} \ 1.64 \text{ ft}.$$

For the present test, two lengths of four feet tubes as shown at the foreground in Figure 41b were used.

Appendix I

PROCEDURES OF ABSORBER AND GENERATOR TEST

Appendix I

A. Preparation

1. The system was cleaned with alcohol and hot water. The liquid circuit was tested to 300 psig and the vapor lines to 250 psig.

2. The system was purged with helium gas and then evacuated for vacuum test.

3. After the vacuum and pressure test, the system was maintained at 83.9 psia with helium gas except the R-22 vapor lines (between the closed valves V10 and V11) which remained evacuated.

4. The weak solution mixing tank was filled with solution with a concentration of R-22 between that of the weak and strong solution.

B. Filling of the System with Solution

1. Introduce solution into the system and the bleed valve on top of the separator is opened gradually to release the helium gas from the system.

2. Observe the liquid level rising in the separator. When liquid appeared at the bleed valve, close the bleed valve and the solution feed valve.

3. Start the pump and close the pump by-pass valve gradually to maintain the reading on the generator inlet pressure gauge at 248 psia and the absorber exit pressure gauge at 83.9 psia.

4. Adjust the absorber weak solution pressure and flow rate by the throttle valve at the recuperator exit and the inlet valve to the absorber.

5. Increase the generator liquid exit temperature to 250°F by adjusting the electrical power input to the heating tapes.

6. Maintain the absorber liquid exit temperature at about 138°F or lower by adjusting the cooling water flow rate with valve V12.

C. <u>Addition of R-22 Vapor</u>

1. As the liquid level in the separator is lowered to midpoint, open the vapor valve to the cooler and the vapor inlet valve to the absorber.
2. Adjust both valves and the coolant flow to maintain the R-22 vapor at the absorber inlet as close to the design condition as possible.
3. If the flow rate is too high, discharge some vapor through the bleed valve on top of separator. If the flow rate is too low, admit R-22 vapor through the vapor charging valve.
4. Adjust pump bypass valve to maintain 83.9 psig at pump inlet and 248 psia at the generator inlet.

D. <u>Operation</u>

1. Adjust absorber coolant water flow rate to maintain strong solution exit temperature at 138.5°F. Record the fluid flow conditions at each component.
2. Maintain proper flow rate at absorber by adding or discharging weak solution or R-22 from the system.
3. Terminate the test when steady state conditions can be maintained for two to four hours.

E. <u>Shut-down of Test System</u>

1. Turn off generator heating input and lower the coolant temperature to the absorber and vapor cooler.
2. As the flow temperature and pressure decrease, open the pump bypass valve gradually to reduce the pressure difference across the pump.
3. Shut off the pump when the generator exit temperature is below 120°F and the pressure difference across the pump is below 20 psi.
4. The system is now ready for additional test runs.

Appendix J

PUMP-TURBINE-MOTOR PACKAGE STUDY

Appendix J

There are two basic types of hydraulic turbines. One type, for example, the Pelton wheel, converts the entire head into velocity so that the fluid is at discharge pressure prior to entering the runners of the turbine. In this type of turbine the runner (wheel) is only partially full of fluid so that its application to the refrigeration system is not possible.

The other type, of which the Francis and Kaplan turbines are examples, converts part of the head into velocity within the runner. The runner must be kept completely full of fluid at all times. For the available head and fluid flow in the weak solution line, the runner would be less than 2.5 inches in diameter and would rotate at speeds in excess of 10,000 rpm. For the refrigerant line, the speeds would be about three times greater. Such small size and high speeds result in lower efficiences, cavitation as well as needs for reduction gear train and flow controls. In short, the turbine is not the most efficient or desirable way to regain energy from the system.

The positive displacement hydraulic motor is much better suited for energy recovery for the flow and head available in the refrigeration system. Well designed units have an efficiency of 83 to 90% depending on type and unlike a turbine, this efficiency varies only slightly over a rather large range of speeds and loads. Furthermore, flow or pressure can be controlled independently by varying the load on the motor. This is due to the fact that at zero speed, the flow is zero except for leakage (flow efficiency is related to leakage) for hydraulic motors whereas the flow through a turbine is almost the same at zero rotation as at operating speeds.

J-1

In the present test system, the mass flow through the refrigerant line is only 5.3% of the total flow whereas 94.7% of the mass flows through the weak solution line. To achieve maximum energy recovery, it is obvious that the hydraulic motor should replace the throttle valve in the weak solution line between the recuperator and the absorber whereas the throttle valve in the refrigerant line between the subcooler and the evaporator should remain. If the motor is mechanically coupled directly to the pump, the total mass flow in the system will depend on pump speed and density of the strong solution as it passes through the pump.

The use of a fixed displacement hydraulic motor located in the weak solution line and coupled directly to the pump assumes that an absorption refrigeration system can operate effectively by close control of the pressure drop between the condenser and the evaporator by use of a throttle valve in the refrigerant line. The volume flow through the refrigerant line would then vary not only with pump speed, but with temperature variations at the motor and pump.

If this situation is not compatible to the refrigeration system, a variable displacement piston motor can be used. In this manner, mass flow can be controlled independently of speed. The penalties imposed by use of a piston motor are an increase in weight by possibly three to four times and a more complicated mechanism both in the control mechanism and motor. Another option is to place a small by-pass line with controlled throttle valve around the motor. This would impose a penalty of loss of energy recovery directly proportional to mass flow through the by pass.

On the other hand, if the hydraulic motor is used to drive an electric generator instead of the pump, greater flexibility of control is achieved. Better control is achieved because either the flow or pressure drop can be controlled independently of any other element of the system. For instance, if a motor-generator set is placed in both refrigerant line and the weak solution line, either can be chosen to control the pressure drop across the condensor and evaporator whereas the other can be used to control mass flow. If it is desirous to control the mass flow through the refrigerant line, then the rotational speed can be monitored and the field coils of the generator can be

LOCKHEED - HUNTSVILLE RESEARCH & ENGINEERING CENTER

controlled to load the motor as necessary to maintain the desired speed. If this mass flow must be some ratio of the mass flow through the pump, then the speed of the pump can be monitored and the resultant signal can be used to control the speed of the motor. The other motor generator set is then used to control pressure in the system simply by controlling the field coils in relation to the measured pressure differences.

In considering angular momentum it can be stated that the electric motor-pump unit plus the fluid in the system can induce angular momentum changes in the space station during changes in operating conditions. By judicious design, it is possible to minimize or eliminate these effects. The hydraulic motor generator units provide flexibility in this regard as the angular momentum imparted to the space station by these units can be used to counterbalance the angular momentum created in the other parts of the system.

The use of generators requires controls and conditioning of the energy so that it can be stored in the storage batteries of the station. It is estimated that the stored energy will be about 65% of the energy saved by the direct coupled method.

Weight increase as a result of motor-generator sets has not been investigated, but a few facts are worthy of comment. First, the size and weight of an electric generator of a given output depends upon rotational speed of the armature. The higher the speed, the smaller the size.

In addition, DC and AC generators must both be considered in order to ascertain the advantages of each for the application. If an AC generator is used, then the weight of a rectifier must be added. The entire question of size, type and control methods must be investigated in order to arrive at the proper course of action.

The question then becomes one of development of a hydraulic motor-pump-electric motor package. It is recommended that this package be considered for development and use in the weak solution line between the recuperator and absorber if two conditions are met. These conditions are 1) the hydraulic losses in the other components of the system are below a predetermined amount and 2) the control system necessary for the successful use of this package is compatible with the operation of the refrigeration system.

The rationale for these conditions are:
1. The hydraulic motor will reduce the electrical power demanded by the pump by about 68% if there are no hydraulic line losses or losses in the absorber. Figure 43 shows the relation between percent power recovered in terms of the electrical power required at the pump and the sum of losses of all other components in the strong and weak solution lines. The minimum acceptable percent power savings will determine the maximum permissible pressure losses. If the losses are less than this amount then the development of the package is justified.

2. The use of the motor will, of itself, not create the required pressure difference in the system, but will only meter the flow. The pressure difference between the condenser and evaporator can be controlled by the throttle valve in the refrigerant line. Thus, pressure in the system is controlled by the throttle valve whereas flow is metered by the motor. If the refrigeration system can operate successfully with this control method, then the package should be considered.

Appendix K

NOMENCLATURE

Appendix K

Symbol

B_o	boiling number
$\dot{C}$	fluid capacity rate
$\overline{C}_p$	specific heat
D	diameter
d_h	hydraulic diameter
G	mass velocity of fluid
h	film coefficient
k	thermal conductivity
L	length
$\dot{m}$	mass flow rate
NTU	number of transfer units
Pr	Prandtl number
Q	heat rate
Re	Reynolds number
r	latent heat of vaporization
S	area
U	overall heat transfer coefficient
V	velocity
x	weight fraction of vapor in liquid
x_{tt}	Lockhart & Martinelli parameter

Greek

Δt	temperature difference
ϵ	effectiveness
μ	viscosity
ρ	density
φ	parameter defined on page H-2

Subscripts

g	gas
i	inside
L, ℓ	liquid
m	log mean value
min	minimum
o	outside or hot wall
s	strong
w	weak or water

Lockheed
MISSILES
& SPACE
COMPANY

In reply refer to:
LMSC-HREC D225034
14 April 1971

National Aeronautics and Space Administration
George C. Marshall Space Flight Center
Marshall Space Flight Center, Alabama 35812

Attention: A&TS-PR-M

Subject: Contract NAS8-25986, Submittal of Interim Report

Gentlemen:

Enclosed is the Interim Report as required under the subject contract. Your
acceptance of this report by return correspondence is requested.

Very truly yours,

LOCKHEED MISSILES & SPACE COMPANY

J. E. Eckert, Contracts
Huntsville Research & Engineering Center

JEE:pgp

Encl: LMSC-HREC D162909, HREC-5986-1, "Evaluation of Absorption Cycle
for Space Station Environmental Control System Application," — Interim
Report, Contract NAS8-25986.

cc: DCASO, DCRA-DBGHP (D. W. VanBrunt)

Distribution:
 See Attached Page

DISTRIBUTION LIST FOR FINAL REPORT UNDER CONTRACT NAS8-25986

Name & Address	Number of Copies
A&TS-MS-IL	1
A&TS-MS-IP	2
A&TS-TU	1
A&TS-PR-M	1
S&E-ASTN-PLB, Mr. Robert Middleton	25
S&E-ASTN-PJ, Mr. Dale Burrows	1
S&E-ASTN-RRI, Mr. Ronald L. Young	1

NASA/Assistant Director for Propulsion
Washington, D. C. 20546
Attn: Mr. A. O. Tischler, OART,
Code RI   1

NASA-Lewis Research Center
21000 Brookpark Road
Cleveland, Ohio 44135
Attn: Mr. Irvin Johnson   1

NASA Scientific & Technical Information Facility
P. O. Box 33
College Park, Maryland 20740   1

Jet Propulsion Laboratory
Liquid Propulsion Section
4800 Oak Grove Drive
Pasadena, California 91103
Attn: Mr. Robert Rose   1

NASA-Manned Spacecraft Center
Houston, Texas 77058
Attn: Mr. Cecil Gibson, Code EP2   1

NASA-Langley Research Center
Langley Station
Hampton, Virginia 23365   1

Mr. R. W. Shivers
Headquarters, Atomic Energy Commission
Germantown, Maryland 20767   1

Dr. L. D. Russell
P. O. Box 85
University of Tennessee
Chattanooga, Tennessee 36403   1